NIWA

Taihoro Nukurangi

Turnover and spawning dynamics of orange roughy on the Northwest Hills, Chatham Rise, 1999

I.J. Doonan, D. M. Tracey, B. Bull,
A.C. Hart, P.J. Grimes

Final Research Report for
Ministry of Fisheries Research Project ORH9801

National Institute of Water and Atmospheric Research

November 2000

Final Research Report

Report title:	Turnover and spawning dynamics of orange roughy on the Northwest Hills, Chatham Rise, 1999
Authors:	I.J. Doonan, D. M. Tracey B. Bull, A.C. Hart, P.J. Grimes
Date:	5 September 2000
Contractor:	NIWA
Project title:	Estimation of the abundance of orange roughy on the Northwest hills on the Chatham Rise (ORH 3B)
Project code:	ORH9801
Project leader:	S. McClatchie
Duration of project:	
Start date	31 December 1998
Completion date:	31 August 2000

Executive summary:

The turnover of spawning orange roughy was estimated on the main seamount in a complex of hills situated on the northwest Chatham Rise to the east of New Zealand. The data used are a temporal sequence of changes in population estimates and the proportions of macroscopic gonad stages. These data were complemented by microscopic examination of the spawning condition of female fish.

No turnover on the Graveyard was found. A model was satisfactorily fitted to the male and female data separately. Spawning begins around 18 to 20 June and dispersal begins between 9 and 16 July. Biomass is constant between these dates. Little can be said about the build up in biomass prior to 17 June because the first survey was not completed until that date. Re-estimating the model using 1996 gonad data with the 1999 biomass estimate on the main spawning hill (Graveyard) gave similar estimated models in which the trajectories of the proportions of gonad stages differed by less than 2 days over a spawning interval of about 20 days.

The microscopic gonad data for females also suggested no turnover. However, these data are not directly linked with the macroscopic staging. The main spawning event begins 18 to 19 June with most fish having started by 28 June. Spawning progresses steadily after 26 June through to 9 July when larger proportions of completely spawned fish are present. The oocyte data also suggests that individuals spawn in a series of batches.

Thus, the models found above can only be used to interpret the spawning dynamics in a coarse way. More work is required to investigate the linkages between microscopic and macroscopic staging.

OBJECTIVES:

Programme objective:

To estimate the abundance of orange roughy (*Hoplostethus atlanticus)* spawning aggregations on the Northwest hills on the Chatham Rise (ORH 3B)

Specific objective:

To investigate the temporal dynamics of orange roughy spawning aggregations on the Northwest hills during the period of the survey, including:

- Turnover of orange roughy on the spawning grounds from the pre-spawning to the post-spawning period.

Introduction

Orange roughy have seasonally synchronised reproduction (Pankhurst et al. 1987), with multiple spawning behaviour apparent within the spawning season (Zeldis, 1993). Aspects of orange roughy reproductive biology and spawning dynamics, such as timing and location, are reasonably well known for New Zealand and Australia (Pankhurst et al. 1987, Pankhurst 1988, Bell et al. 1992, Zeldis et al. 1997a). More poorly defined is the smaller scale variability within spawning, how the spawning mass builds up for spawning and declines afterwards, and whether there is turnover of fish during the spawning period.

Turnover is part of the spawning mass build up and decline cycle and can occur through groups of fish arriving on the grounds at different times or leaving at different times once they have spawned, i.e., only a portion of spawning fish is present at any one time. Abundance analyses for orange roughy using acoustics or egg survey methods often implicitly assume that all spawning fish are in the survey area at the same time, i.e., no turnover. However, if turnover exists, then a downward bias is introduced into any absolute abundance estimates from acoustic surveys. For egg surveys, turnover could give biases of a different signal depending on the nature of the turnover. For fish leaving during the trawl survey period, (trawling is required to obtain the fecundity data), the biomass estimate will be over-estimated. For fish that both arrive and leave either before or after the survey period, the biomass is under-estimated (Zeldis et al. 1997a). Information on spawning dynamics is also of importance to understanding populations of exploited fish which, in turn, is needed to construct appropriate management models.

Previously, whether turnover has been occurring was assessed by using macroscopic gonad staging and tracking the decline in the proportions of pre-spawning fish as well as the build up in the proportion of spent fish over time (e.g. Zeldis et al. 1997a, Francis et al. 1997). Zeldis et al. (1997b) found that turnover of spawning orange roughy had occurred during the 1993 and 1995 egg surveys at Ritchie Bank but not at East Cape in 1995 (Figure 1). Applying this same method turnover was also found not to have occurred in the 1996 egg survey of the Northwest Hills seamount complex on the Chatham Rise (Figure 1) (Francis et al. 1997). The conclusion drawn from these studies was that turnover, when it exists, takes the form of spent fish leaving the grounds prematurely, perhaps caused by commercial fishing (Zeldis et al. 1997a, Francis et al. 1997). However, gonad stage proportions can be ambiguous to interpret, e.g., a constant spent proportion with time can be caused by spent fish moving away, mature and ripe fish moving in, or a mixture of both. Knowing the relative biomass through time helps to resolve such ambiguities.

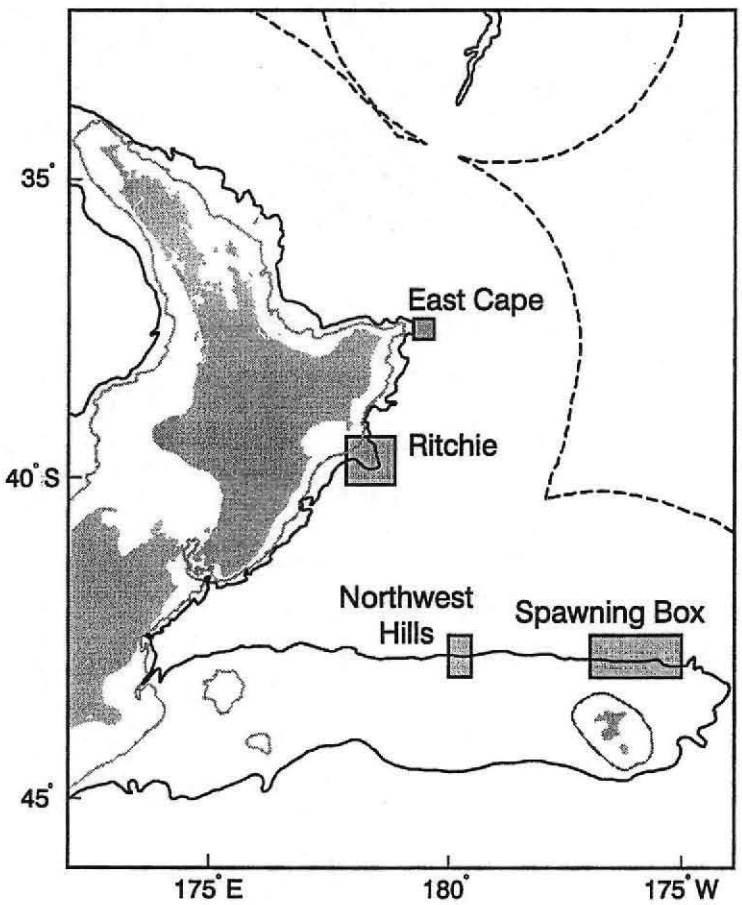

Figure 1: Map showing location of main study area (Northwest Hills), other areas where turnover has been investigated (East Cape and Ritchie), and main spawning site on the Chatham Rise (Spawning Box).

Turnover and spawning dynamics of orange roughy were investigated during spawning on the Northwest Hills seamount complex in June and July, 1999. Data used were from the acoustic surveys and trawling (voyages TAN9908, AEX9901, and SRA9901). Two vessels were used during the main survey so that the acoustic surveys could continue unimpeded by the extensive trawling that was needed. The vessels used were the NIWA vessel, *Tangaroa,* and a commercial fishing vessel, *Amaltal Explorer* owned by Amaltal Fishing. An additional commercial vessel, *San*

Rangitoto, (Sanford Ltd) gathered further samples from trawling 8 days after the end of the main survey.

The Northwest Hills comprise a complex of 10 major seamounts which are generally separated from each other by gently sloping seafloor just east of 180° longitude on the north Chatham Rise (Figure 2). The surrounding flat ground is at 900–1200 m, but the seamounts rise up to 200–350 m above it. Other minor geographical features are also present in the area but these are much smaller than the main seamounts (Wood et al 2000). Spawning takes place in large aggregations over some of these seamounts in late June and early July, which is slightly earlier than that for the Spawning Box, the nearest known other spawning site, (Figure 1), for which spawning occurs in mid to late July.

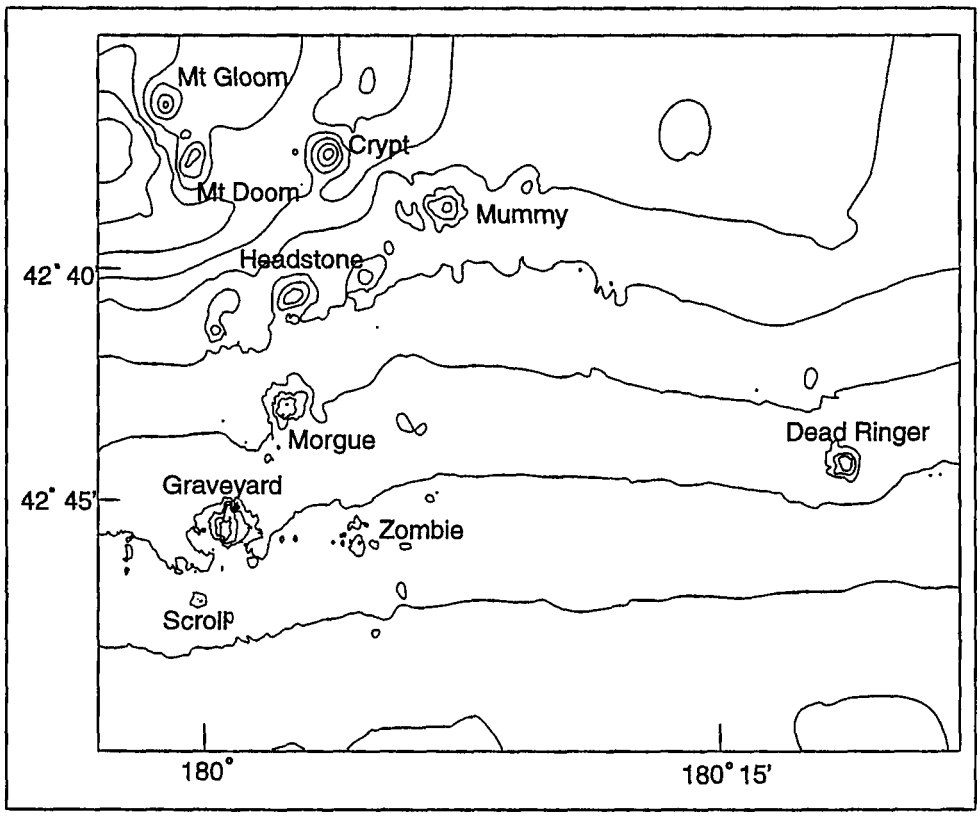

Figure 2: 100 m interval contour plot of the Northwest Hills complex showing the locations of main hills.

The original intent for the turnover study was to survey 5 seamounts that had been shown to have the most significant marks in an acoustic survey in 1997 (Bull et al. 1999). However because species composition data from trawling were not available for all seamounts surveyed in 1997, the marks used in the analysis were assumed to mostly comprise orange roughy. These marks proved deceptive as when the hills were re-surveyed in 1999, the species composition was different to that assumed earlier, with. other species contributing to the marks on some of the seamounts. One seamount, the Graveyard, had 83% of the spawning recruited biomass of the 5 seamounts, and 76% of the total for all seamounts (Bull et al. 2000). Hence, the

analysis for the turnover experiment was restricted to the Graveyard seamount only. Data for the Graveyard were also the most complete in terms of macroscopic gonad stages.

For the Graveyard seamount, it was postulated that there would be a build up in population size which reaches a plateau, and then declines as orange roughy disperse after spawning; corresponding to fish arriving in pre-spawning condition, spawning, and then leaving in a spent condition. The underlying assumption was that fish arrived, spawned, and left the Graveyard with some degree of synchrony. The intent of this study was to describe the temporal build-up and subsequent decline of a spawning aggregation rather than to attempt to explain the mechanisms driving it (e.g. by relating aggregation density to some environmental variables).

Population size build up and decline was investigated through a series of biomass estimates carried out at semi-regular intervals during spawning. These estimates, along with the trend in the proportions in macroscopic gonad stages over time, were used to model turnover and spawning dynamics. Males and females were analysed separately. The model used a simple mechanism whereby the rate of fish developing from one gonad stage to the next was proportional to the amount of fish in the earlier stage. Knowing the biomass trend and the pattern of change in the proportions of gonad stages allowed the estimation of rate parameters, including the rate of fish coming into the area and the rate of those leaving. The latter two parameters control the extent of turnover and if there was no turnover, they are zero in some central period, when the biomass is stable.

Supporting evidence came from examining ovary sections microscopically. Microscopic examination can give a more precise understanding of female spawning dynamics and can also enable counts of the numbers of oocytes. These data are more reliable than the macroscopic staging at defining the transition period during spawning between the fully-established stages.

Significant fluctuations in the frequency of post-ovulatory follicles (POF's) in the ovary over time (effectively a measure of percent spawned for an individual at the time of sampling) indicates turnover from different groups of fish spawning out-of-phase. Depending on whether turnover is suggested or not, analysis of daily changes in the proportion of post-ovulatory follicles will enable the determination of the timing of spawning during July (both onset and tailing off or completion). Bell et al. (1992) showed that with orange roughy in Australian waters, post-ovulatory follicles do not degenerate until early August after a main spawning period in June/July. Hence, there is confidence that the post-ovulatory follicles would be still countable during the July spawning period in the survey area.

Methods

Biomass surveys

In the original design, the turnover experiments had a total of 8 grid surveys including the abundance survey as grid 4. The NIWA *CREST* system and towed body were used to survey the major hills, Graveyard, Scroll, Morgue, Zombie, Headstone (2 transects each, crossing over the top of the seamount) and the near flat ground from 800 to 1200 m (3 transects). The survey grid over the hills is shown in Figure 3. The course was designed to reduce the number of turns necessary and hence the time expenditure. The towed body was used for the acoustic sampling. The towing speed was 3–6 knots over the hills (depending on the depth of the hills) and 5–6 knots over the flat. The towed body depth was around 200 m over the marks.

Analyses were restricted to the Graveyard hill where the main spawning aggregation was present. There were also more biomass estimates for the Graveyard because the diurnal experiments were located on this hill (Bull *et al.* 2000). In addition, consistent catches of spawning orange roughy were made on Graveyard, whereas most other hills yielded many misses or infrequent catches that tended to consist of smooth oreo and non-recruited or non-spawning orange roughy. The exception to this was that consistent aggregations of spawning orange roughy occurred to the south of Graveyard on the seamount Scroll.

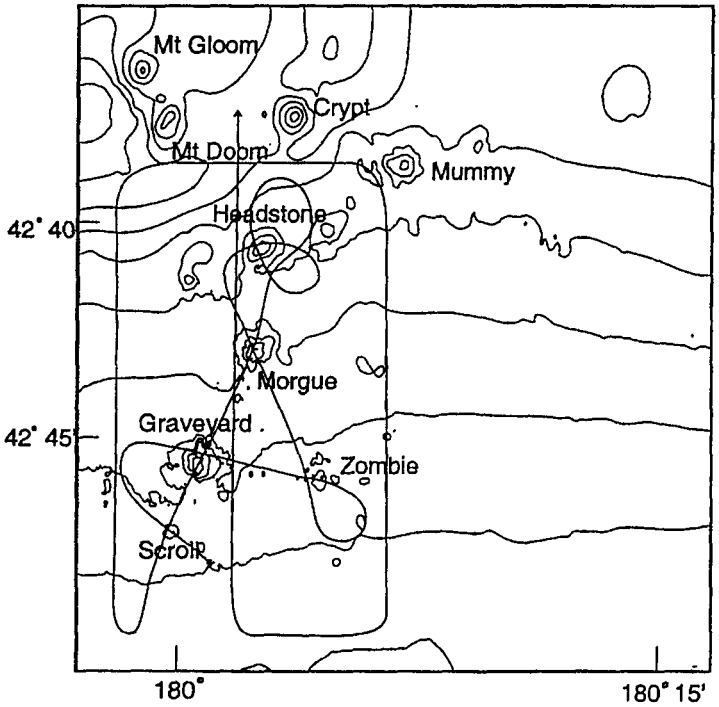

Figure 3: Example of hill and central flat track for the grid surveys (turnover experiment).

There were 12 estimates of biomass on the Graveyard from the following sources:

- Grid surveys, six estimates on the Graveyard
- The biomass survey which surveyed the Graveyard along with all other seamounts and the surrounding flat ground to estimate biomass for the whole Northwest Hills and surrounding area. The trawl data were restricted to those tows carried out at the time of the survey. This gave a figure that was slightly different to that reported in the biomass survey due to a different subset of trawl data being used. The survey estimate was 2590 t.
- Diurnal experiments, where the Graveyard was acoustically surveyed on 4 days in a 5 day period. Biomass estimates were made for each day. No trawls were carried out on Graveyard during this experiment so trawl data from trawls just prior to and after the experiment were used.
- Visual. Eight days later when additional samples were collected from the Graveyard on the *San Rangitoto,* a visual estimate, relative to the size of the marks during the survey, was made (D. Tracey, pers. comm.). Supporting evidence for this estimate came from the difference in catch rates of orange roughy during the main survey period (means for the Tangaroa and Amaltal Explorer were 62t and 331 t / n. mile respectively) compared to those from the *San Rangitoto* (21 t/n.mile). Additionally, one trawl by the *San Rangitoto* was made along almost the entire side of the hill which was not even attempted in the main survey for fear of breaking the trawl gear. For variance purposes, a sample size 0.5 transects was assigned.

Biomass was estimated for spawning recruits (gonad stage 3 or more, length 32 cm or more) and used the over-sampling correction (Bull et al. 2000) to compensate for the star design of the transects. Species composition and length and gonad data came from trawl catches.

The *c.v.* for each Graveyard biomass estimate was given by 0.5/sqrt(n), where n was the number of transects and 0.5 is the sampling *c.v.* of the mean backscatter on a transect. The latter was estimated separately for data outside the diurnal experiment and for data from the diurnal experiment. Both gave 0.50. Error from the species composition was ignored because the biomass results in Bull et al.(2000) showed that 99% of catch was orange roughy and 1% was Baxter's dogfish (*Etmopterus baxteri).* Sampling error in the target strength of orange roughy was not considered because this error is cancelled out when comparing trends in the biomass (this is how the turnover analysis uses biomass). The variance of the estimate of biomass from the spawning turnover model would require the target strength error to be added on to it after the analysis.

The biomass was divided into male and female parts. As the male ratio in the trawls showed no trend over the spawning period, the average ratio was used, .i.e., 0.685 (*c.v.* 7%). The key with the biomass in this analysis is the relative changes over time and because of the constant sex ratio this means that both sexes change in the same way. Although nothing is explicitly gained by splitting biomass by sex, the trends in the gonad stages are different enough between the sexes to warrant separate analyses. The *c.v.* for the male and female biomasses was given by

$\sqrt{\{ (1 + 0.5^2/n)(1 + 0.07^2)-1 \}}$

The biomass values are given in Table 1 and Figure 4.

Table 1: Graveyard male and female biomass, source, date, transects and c.v. Biomass at each date was estimated independently of those on other dates. Population c.v. was 50%

Source	Date	Days since 31 May	Number of transects	Biomass		c.v.
				Male (t)	Female (t)	(%)
Grid 1	17 June	17	2	2 500	1 100	35
Grid 2	18 June	18	2	1 200	550	35
Grid 3	21 June	21	2	1 700	800	35
Biomass survey	24 June	24	4	1 800	830	25
Grid 5	27 June	27	2	2 000	920	35
Grid 6	2 July	32	2	2 100	990	35
Diurnal 1	4 July	34	16	2 200	1 000	13
Diurnal 2	5 July	35	15	2 200	990	13
Diurnal 3	7 July	37	16	3 000	1 400	13
Diurnal 4	8 July	38	16	2 200	1 000	13
Grid 8	9 July	39	2	2 100	980	35
Visual	17 July	47	0	410	190	71

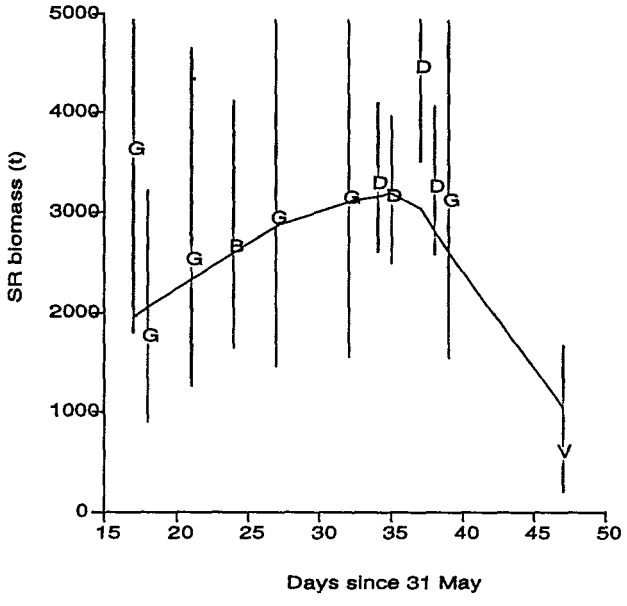

Figure 4: Orange roughy biomass of spawning recruits by days since 1 June. Vertical bars are +/- 1 standard errors, except that the upper part is truncated at 5 000 t. Data sources are indicated by: "G" = grid survey, "B"= biomass survey, "D"=diurnal experiment, "V"= visual estimate. Line is a smooth ("lowess") through the data.

An alternative method of estimating biomass was also tried. In this method the transect means were adjusted by a factor for the direction of the transect (Appendix 1). This factor was estimated from the diurnal experiment data and assumes that the mark distribution is more or less stable through time, which was the

case in the diurnal experiment. This method changes most biomass estimates a little, but with two changing by 20% to give a flatter trend than the usual method (Table 2, Figure 5). The sample *c.v.* for the mean backscatter was estimated as 40%.

Table 2: Alternative Graveyard male and female biomass, source, date, transects and c.v. Biomass at each date was corrected for the effect of the transect direction (which was estimated in the diurnal data). Population c.v. was 40%

Source	Date	Days since 31 May	Number of transects	Biomass		*c.v.*
				Male (t)	Female (t)	(%)
Grid 1	17 June	17	2.0	2 500	1 200	28
Grid 2	18 June	18	2.0	1 300	600	28
Grid 3	21 June	21	2.0	2 100	980	28
Biomass survey	24 June	24	4.0	1 600	740	20
Grid 5	27 June	27	2.0	2 100	950	28
Grid 6	2 July	32	2.0	1 800	850	28
Diurnal 1	4 July	34	16.0	2 100	950	10
Diurnal 2	5 July	35	15.0	2 300	1 000	10
Diurnal 3	7 July	37	16.0	3 200	1 400	10
Diurnal 4	8 July	38	16.0	2 100	950	10
Grid 8	9 July	39	2.0	2 400	1 100	28
Visual	17 July	47	0.5	410	190	57

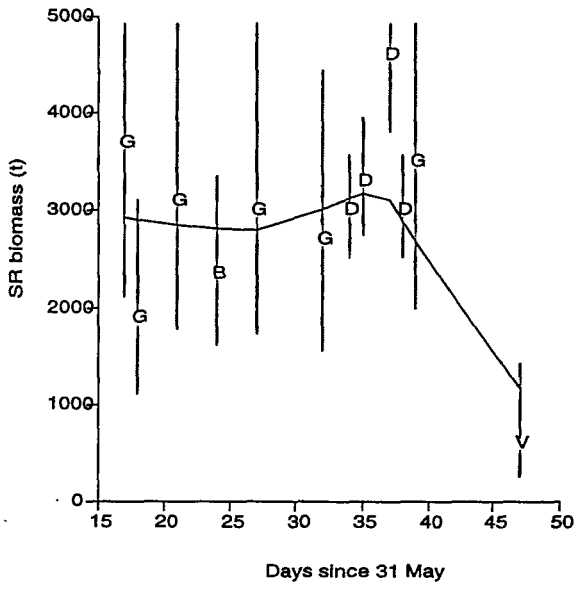

Figure 5: Alternative biomass method, transect direction factor method for biomass. Orange roughy biomass of spawning recruits by days since 1 June. Vertical bars are +/- 1 standard errors, except that the upper part is truncated at 5 000 t. Data sources are indicated by: "G" = grid survey, "B"= biomass survey, "D"=diurnal experiment, "V"= visual estimate. The line is a smooth ("lowess") through the data.

Biological sampling

Fish were caught by the *Tangaroa* with a rough bottom orange roughy trawl (100 mm codend) on the hills and a wing trawl (ratcatcher) with 40 mm codend on the flat. *Amaltal Explorer* used a Champion 2 panel trawl without lower wings for hill fishing (100 mm mesh codend) and for fishing on the flat the same trawl was used but with lower wings and a squid codend (60 mm mesh). Flat trawls were targeted on any heavier marks seen along the transects. These tows were north-south and covered the length of the mark, up to 1.5 nm. When no notable marks were seen, tows were evenly spaced over depths (between 800m and 1500m).

The catches from each successful tow on both vessels were sorted and weighed by species to the nearest 0.1 kg. For catches too large to be weighed, the total greenweights for orange roughy were back-calculated to total catch weight from a greenweight-to-product weight conversion factor. For large catches, at least three samples of 200 orange roughy were taken from different parts of the net to ensure sampling was representative of the catch. A random sample was selected from each tow and staged length frequencies (standard length to the nearest mm below), sex, and gonad stage data collected. Gonads were macroscopically staged following the system of Pankhurst *et al.* (1987), with the addition of a partially-spent stage (Zeldis *et al.* 1997a) and are summarised below.

Macroscopic Stage	Female	Male
1	Immature/Resting	Immature/resting
2	Early maturation	Early maturation
3	Maturation	Maturation
4	Ripe	Ripe
5	Running ripe	Spent
6	Spent	–
7	Atretic	–
8	Partially spent	Partially spent

Additional staged length frequency data and gonad samples were also collected from the Graveyard hill on the 47th day by *San Rangitoto*.

For spawning dynamics, only the male gonad stages 3 (Mature), 4 (Ripe), and 5 (Spent) and the female stages 3 (Mature), 4+5+8 (Ripe), and 6 (Spent) were used. Proportions were formed by sex, covering the mature, ripe and spent stages (Figure 6). Samples were included only if the total catch was over 500 kg (lower catches tended to be missed trawls and unrepresentative of fish in the mark) and the fish sample size was 10 or more.

For comparison, Graveyard trawls carried out in conjugation with an egg survey in 1996 to estimate the biomass of orange roughy (voyage TAN9608), were also plotted (Figure 7). Proportions in each gonad stage over time were similar between the two datasets. However, the male ratio in the catches was reversed, 70% males in 1999, 30% in 1996.

For males, both years data show a similar pattern in the trends of the gonad stages proportions. Mature proportions decline from nearly 100% to zero and spent proportions rise from zero to nearly 100%. Ripe proportions rise and fall with the peak appearing earlier by a few days in 1999 compared to 1996.

The pattern in the female stages have some differences to the male one and there are also some slight differences between the years. Mature proportions only start at about 50% before declining to zero and spent proportions rise from zero to about 90%. The ripe proportions (stages 4&5) are roughly constant, declining in the last trimester. In 1996, the proportions of stage 4 are always far higher than those for stage 5, but in 1999, this pattern only existed initially before reversing later on. No reason is apparent for this difference between years, unless it is due to the reversal in the sex ratio of the catches in the two years indicating that different parts of the female population were sampled.

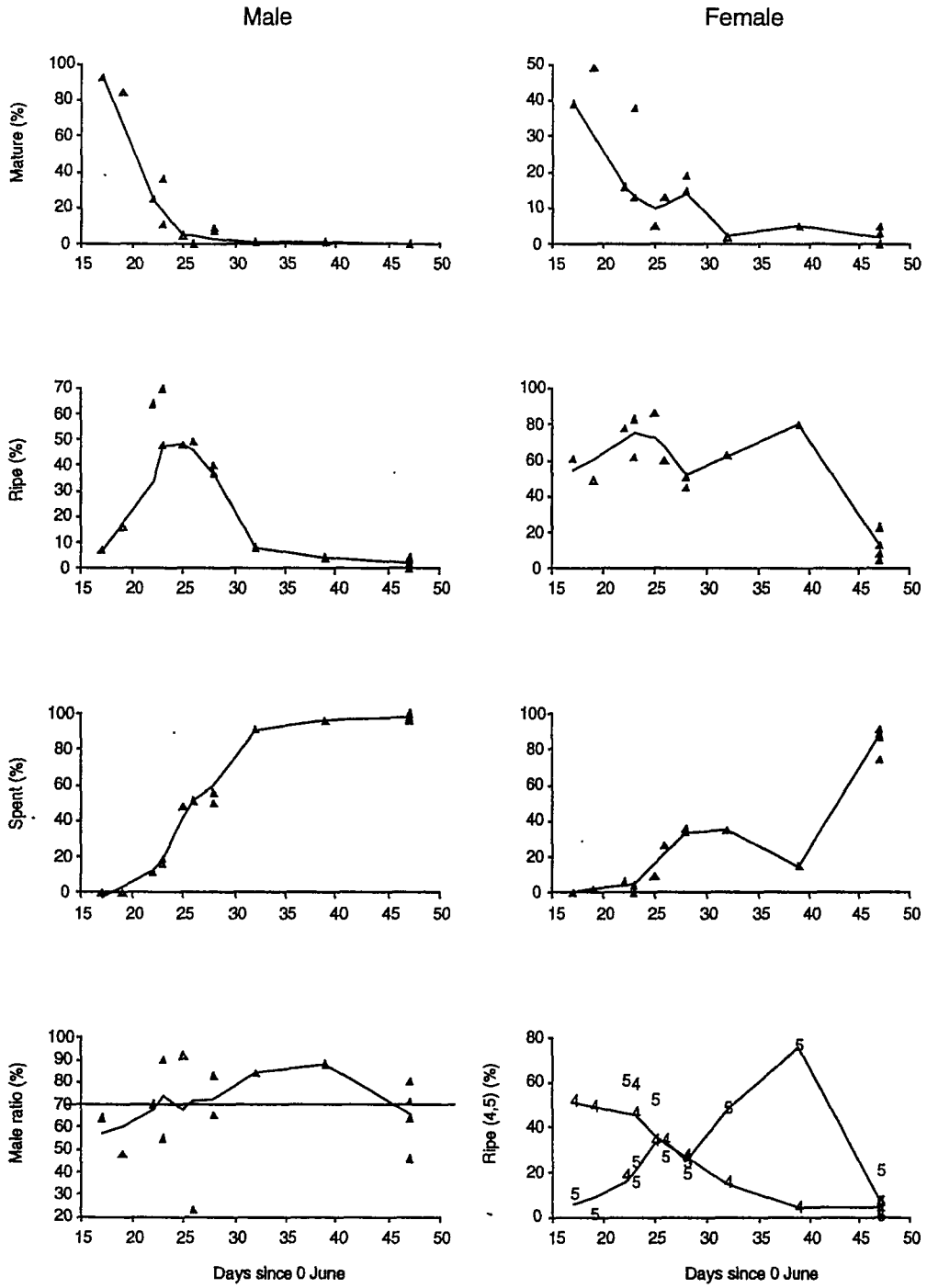

Figure 6: Male and female macroscopic gonad stage proportions and the male proportion in the catch by days since the start of June (Graveyard 1999 data). Also shown are smooth curves through the data (S function "lowess"). The horizontal line in the male ratio plot is the mean ratio over all the data. The bottom right hand plot separates the female ripe (4) and running ripe (5) stages.

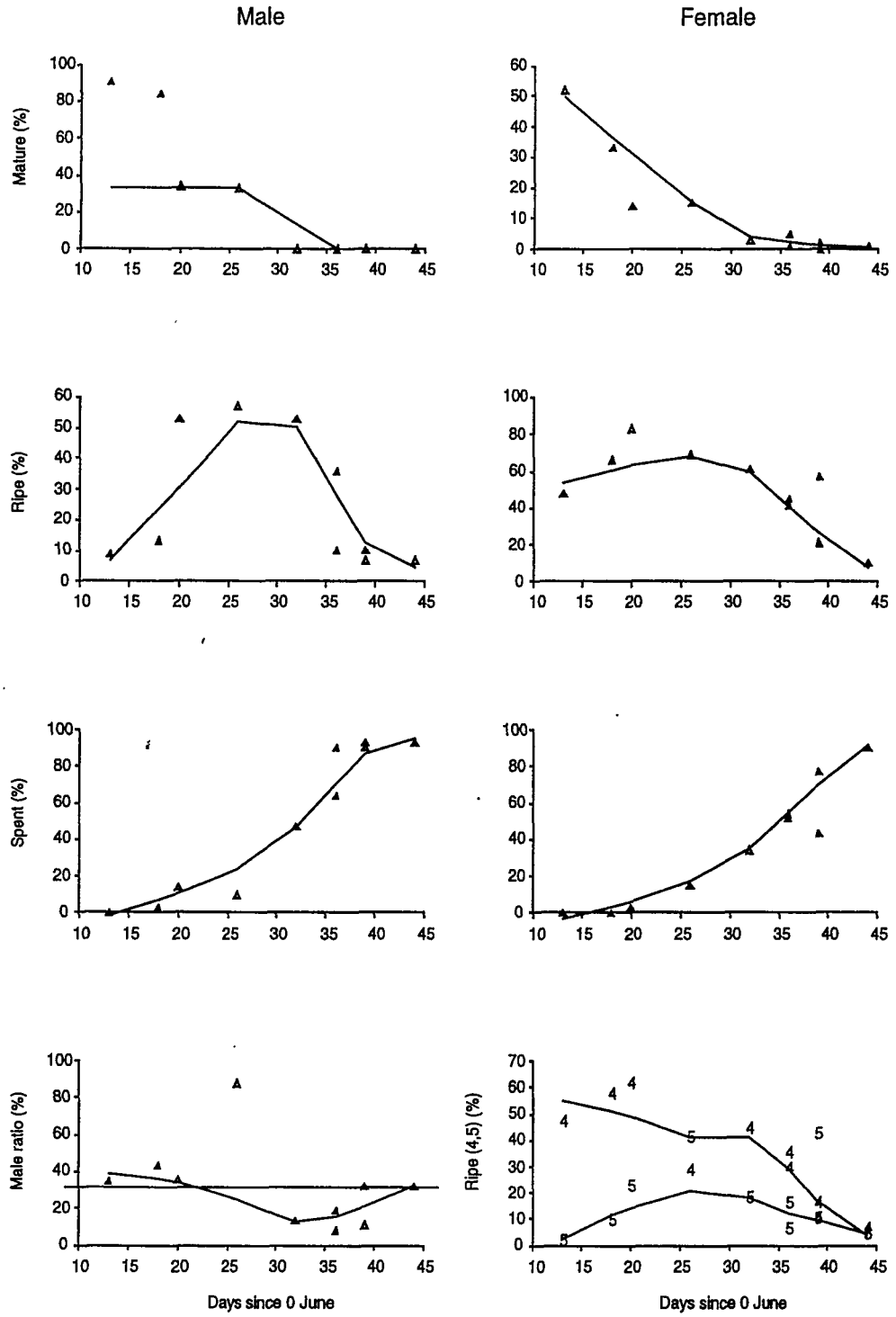

Figure 7: **Male and female macroscopic gonad stage proportions and the male proportion in the catch by days since the start of June (Graveyard 1996 data). Also shown are smooth curves through the data (S function "lowess"). The horizontal line in the male ratio plot is the mean ratio over all the data. The bottom right hand plot separates the female ripe (4) and running ripe (5) stages.**

Histological counts

Up to 100 female fish were randomly sampled per day to obtain histological samples. Gonad samples were primarily taken from Graveyard seamount (the main spawning hill) plus Scroll, Deadringer and Wecnec. The Graveyard was sampled every 2–3 days during the course of the survey. Ovary samples were for fecundity estimation and histological analysis and so individual fish were weighed prior to removal of gonads.

The histological collection procedures followed those used during previous egg production surveys (Zeldis *et al.* 1997a,b; Francis *et al.* 1997). For 50 gonads, several sections were taken along the length of the ovary to check on variation in oocyte development with and between gonads.

Gonads were removed and left connected at the posterior end by the external vent tissue to minimise the loss of eggs during preservation. Gonad sections were collected using 2 methods.

1) a thin slice of the entire cross-section of the middle of 1 fresh ovary (see Figure 8) was placed in a cassette and the cassettes were placed in container with 10% fresh formalin in seawater.
2) the 2nd fresh uncut ovary was fixed in 10% formalin. This gonad was injected with an amount of 10 % formalin equal to half the volume of the gonad and left for 12–24 hr. The middle of the ovary was then sectioned and placed in jar of 10% formalin.

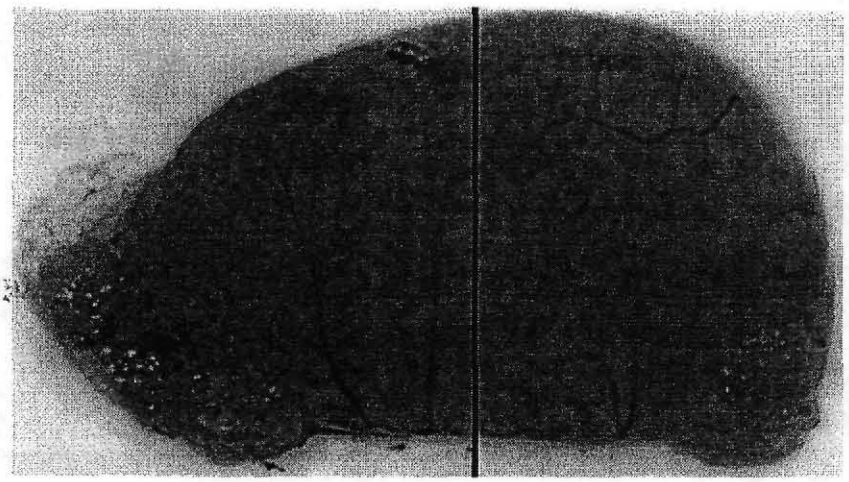

Figure 8: Female orange roughy ovary (stage 4) showing position of the thin slice cross-section.

For the microscopic study, ovary samples were processed in the laboratory, embedded in paraffin, sectioned at 4μm, and stained with haemotoxylin and eosin preparations. The sections from each ovary were examined using transmitted light under a binocular microscope. Counts to provide the total number of post-ovulatory follicles as well as the total number of active oocytes (stage 4 and stage 5), were made. Identification of the histological condition stages of gonads of female orange roughy followed Pankhurst *et al.* (1987) and is summarised below for females stages 4–6.

Microscopic Stage for oocytes	Histological condition
4 (hydration)	Final oocyte maturation; nuclear migration and breakdown; coalescence of yolk material and oil droplet formation.
5 (ovulation)	Follicular separation and rupture
6 (spent)	Post-ovulatory follicles, increased vascularizarion, follicular atresia

Oocyte stages and post-ovulatory follicles are shown in Figures 9 a-c. Stage 4 (GVM) oocytes show nuclear migration and breakdown, coalescence of yolk material, and oil droplet formation. Stage 5 (M) oocytes show follicular separation and rupture. Where post-ovulatory follicles (POF) were dominant increased vasculaization and follicular atresia is seen.

The appearance of postovulatory-follicles is a clear sign that the fish has started to spawn (releasing oocytes). As spawning develops, the proportion of post-ovulatory follicles will increase, and the amount a fish has spawned can be estimated. The ratio of post-ovulatory follicles to other oocyte stages (vitellogenic, hydrated, ovulated) can also indicate how synchronised oocyte development, and hence egg release, is in a single fish, as well as over the wider population.

The distribution of the fraction of post-ovulatory follicles and mature oocytes were examined by location, and over time.

About 2000 ovary samples were collected for histological examination of oocyte development and changes in frequency of oocyte stages over the period of the survey.

Fifty sets of gonads were sectioned as planned to study between- and within- ovary variation in oocyte development. No difference between section site was noted. Neither was there a difference between the 2 methods of fixing sections. Post-ovulatory follicle and oocyte counts were similar when comparing sections taken from fresh ovaries with sections taken from the ovaries that had been fixed for at least 24 hours.

As spawning progressed the abundance of stage 4 and 5 oocytes decreased as the proportion of post-ovulatory follicles increased. Recovering ovaries with post-ovulatory follicles not present were at stage 2. A small number of stage 3 (exogenous vitellogenesis) oocytes were noted during histological examination but not counted.

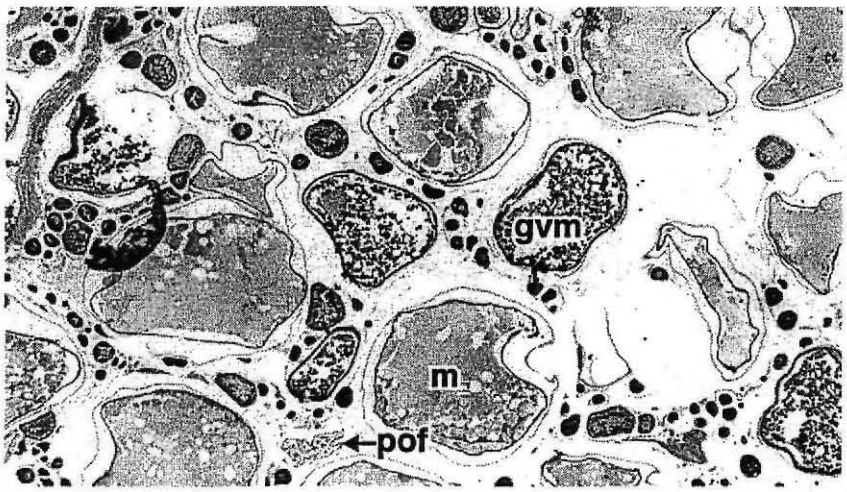

(a)

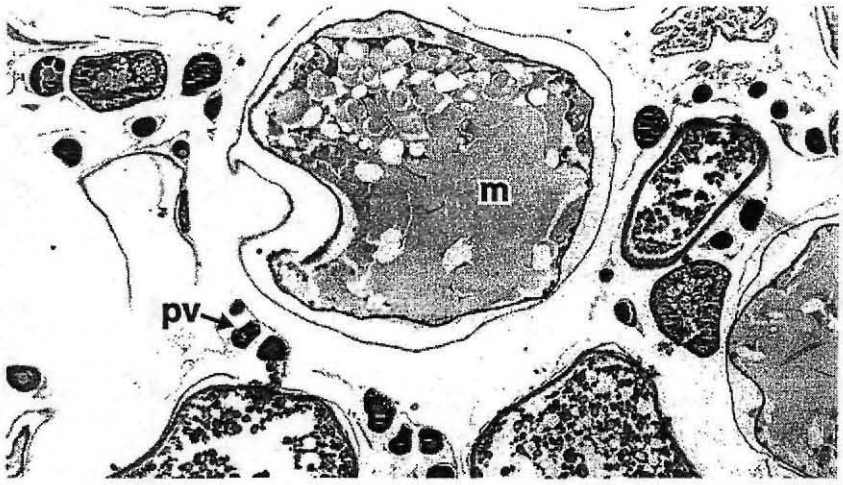

(b)

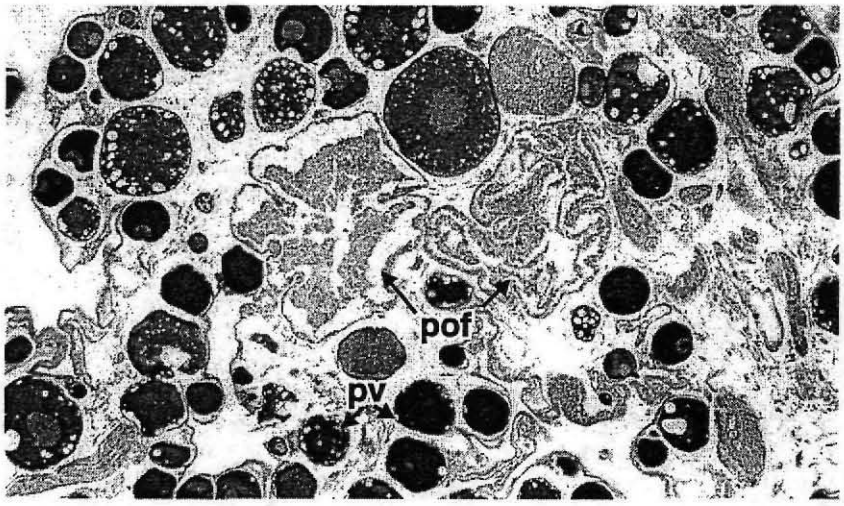

(c)

Figures 9 (a-c) Photographs of sections from orange roughy ovaries showing (a) final maturation oocytes (gvm) (b) mature oocytes. (m) and (c) post-ovulatory follicles (POF). (Note: pv are oocytes that are previtellogenic (immature)).

Spawning dynamics and turnover model

The spawning dynamics were analysed using a linear compartmental model following Seber and Wild (1989). This method assumes that there are a finite number of sub-systems (compartments) which are homogeneous and well mixed and that interactions between compartments is by exchange of materials. Inputs from outside the system can go into one or more of the compartments, and outputs from the system to the outside can also occur from any of the compartments. The rates of transfer between compartments are linear, i.e., the rate from compartment i to j is proportional to the current amount of material in i. The first use of these models was for the transport of tracers through animals and humans in the 1940's.

Our use of compartmental models for spawning requires a re-orientation of terms (Figure 10). Here, "material" is the biomass of fish in each of 3 spawning states. These states (macroscopic) are mature, ripe, and spent. Females have an additional state, running ripe (5) and so to keep females to three states, ripe (4) and mature (3) were combined so that "ripe" in the model was running ripe stage. Spent was made up of stages 5 and 8 for males, and stages 6 and 8 for females. The transfer rates relate to moving from one spawning stage to another and not to a physical movement from one place to another. The system was the spatial confines of the spawning hill, Graveyard, i.e., the fish in each state were not necessarily spatially separated, as in the classic applications of the compartmental model. "Inputs" are flows of fish in the ready stage moving onto the Graveyard. "Outputs" are spent fish moving off the Graveyard. Appendix 2 gives the theory of compartmental models for this application.

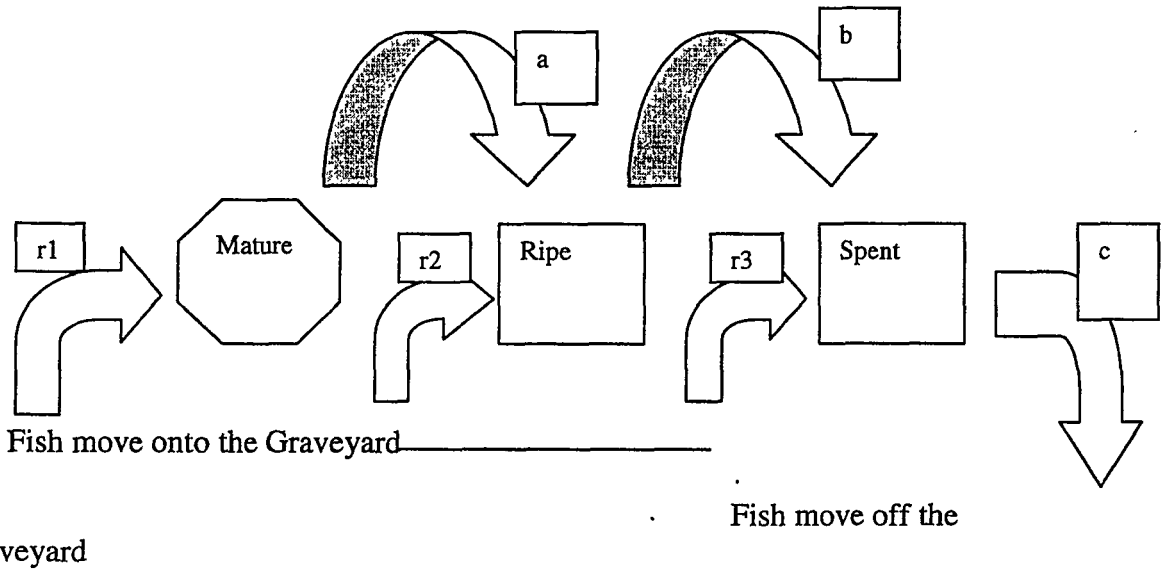

Figure 10: Three stage spawning compartment model. Arrows show direction of flow with the symbol for the transfer rate above each.

Because the preliminary data showed different patterns for females and males, the data from each sex were analysed independently.

The spawning dynamics (Figure 10) are given by the following equations;

$$\frac{\partial}{\partial t} f_{Ready} = r1 - a f_{Ready}$$
$$\frac{\partial}{\partial t} f_{Ripe} = r2 + a f_{Ready} - b f_{Ripe}$$
$$\frac{\partial}{\partial t} f_{Spent} = r3 + b f_{Ripe} - c f_{Spent}$$

where f denotes biomass, t is time (days), r's are constant rates of fish moving onto the Graveyard (t.day^{-1}), a, b, and c are constant transfer rates (day^{-1})
Given that $a \neq b \neq c > 0$, the solutions are (Appendix 4):

$$f_{Mature} = \{B_M - r1/a\} e^{-at} + r1/a$$

$$f_{Ripe} = \left\{(B_M - r1/a)\frac{a}{b-a}\right\} e^{-at} + \left\{\frac{a(B_M - r1/b)}{(a-b)} + (B_R - r2/b)\right\} e^{-bt} + (r1+r2)/b$$

$$f_{Spent} = \left\{(B_M - r1/a)\frac{ab}{(b-a)(c-a)}\right\} e^{-at} + \left\{\frac{(B_M - r1/b)ab}{(a-b)(c-b)} + (B_R - r2/b)\frac{b}{c-b}\right\} e^{-bt} + \left\{\frac{ab(B_M - r1/c)}{(a-c)(b-c)} + \frac{(B_R - r2/c)b}{b-c} + (B_S - r3/c)\right\} e^{-at} + (r1+r2+r3)/c$$

where B_M is the mature biomass at the start, B_R is the ripe biomass at the start, and B_S is the spent biomass at the start.

If c is zero, then f_{Mature} *and* f_{Ripe} are the same as above, but f_{Spent} is given by

$$\left\{(B_M - r1/a)\frac{b}{(b-a)}\right\}(1 - e^{-at}) + \left\{\frac{(B_M - r1/b)a}{(a-b)} + (B_R - r2/b)\right\}(1 - e^{-bt}) + (r1+r2)t + B_S$$

Although rates must be constant, this only needs to apply within a time interval. Different intervals can have different rates. Thus, spawning can be approximated by a sequence of time intervals where the starting biomasses in one interval are the biomasses at the end of the preceding interval. These are used for at least three

intervals. The simplest scenario is when there is no turnover (Figure 11). The first interval is pre-spawning so that $a = b = c = 0$ and $f_{Mature} = B_M(0) + r1 * t$, where $B_M(0) = B$ is the biomass on the Graveyard at time 0 (taken as the start of June). The second phase, spawning, starts at time, t_c. Then, $a \neq b > 0$, $c=0$ and the biomasses are given by the second solution given above. The third phase starts at time, t_{c2}, when all fish disperse from the Graveyard at the same rate *(c2)*. The biomasses are given by a generalized version of the first solution above.

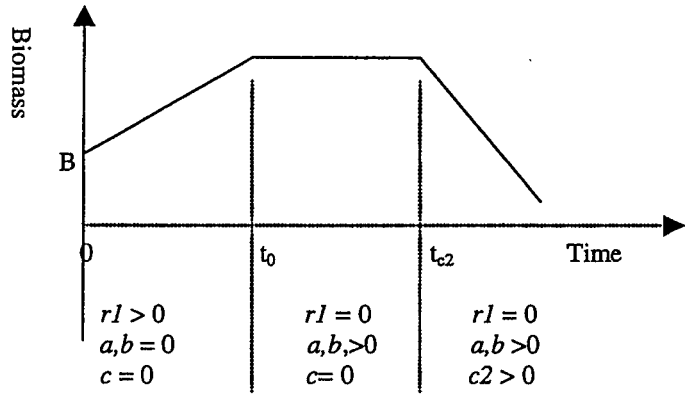

Figure 11: Simplest spawning dynamics, no turnover using 3 phases. *r2 = r3* =0.

A more complicated scenario is given in Figure 12 where mature fish are still arriving on the Graveyard after spawning starts, and then sometime later, spent fish leave before the general dispersal phase. Phases 2 and 3 are solved by the second solution above, and phase 3 would use the first solution above. The full list of parameters used is given in Table 3.

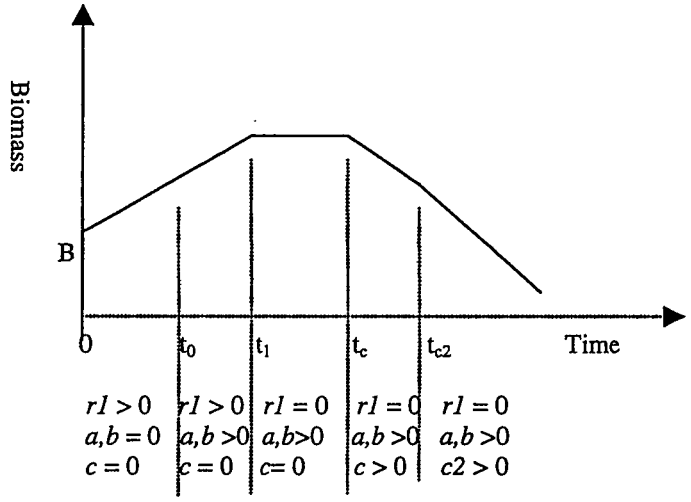

Figure 12: Spawning dynamics using 5 phases. *r2 = r3* =0.

Table 3: Parameters used in the spawning dynamic model. Time is measured as days since 1 June

Parameter	Meaning
t_0	Time when spawning starts
t_1	Time when fish stop moving onto the Graveyard after t_0 Optional parameter, set to t_0 if not being used
t_c	Time when spent fish start moving off the Graveyard Optional parameter
t_{c2}	Time when dispersal phase starts and all fish start to move off the Graveyard
ta	Time when transfer rates switch from *a, b* to *a2, b2.*
r1, r2	Rates of biomass (mature, ripe) moving onto the Graveyard Operates from time 0 to t_1
a,a2	Transfer rate of mature fish into the ripe gonad stage Operates from time t_0
b,b2	Transfer rate of ripe fish into the spent gonad stage Operates from time t_0
c	Rate of spent fish leaving the Graveyard Operates from time t_c to t_{c2}
c2	Rate of all fish leaving the Graveyard during the dispersal phase Operates from time t_{c2}
B	Biomass on the Graveyard on day t_0 (all mature fish)

Objective function

For each sex separately, the model was fitted to the two types of observation, assumed to be independent, using weighted least squares. The objective function to be minimised was

$$F = F_{abd} + pen * F_{GS}$$

where F_{abd} is the value given by the fit to the total abundance data , F_{GS} is the value from fitting to the proportions of fish in the different gonad stages (mature, ripe, and spent), [Note: This takes into account sampling variation between trawls as well as variation within the orange roughy sample or subsample within the trawl] The objective function *pen* is a penalty used to control the relative contribution from F_{abd} and F_{GS}.

For the abundance estimates,

$$F_{abd} = \sum_{i}^{nb} \left(B_i - \left(f_{Mature}(t_i) + f_{Ripe}(t_i) + f_{Spent}(t_i) \right) \right)^2 / \sigma_i^2$$

where B_i is the estimated total abundance, *nb* is the number of abundance estimates, t_i is the number of days from the 31 May that B_i relates to, and σ_i is the standard deviation in the log scale for the abundance estimate. If B_i was log-normally distributed and σ_i known, then F_{abd} is the log-likelihood up to a constant. σ_i was estimated from the sampling variance of the estimated B_i's.

For the gonad stage data (F_{GS}), the proportions were treated as logistic-normal variants (Aitchison1983), rather than multi-nominal, which allows for extra variation in the mean proportions between trawls than that given by the multi-nominal

distribution. Between trawl variation is usually the major source of variation so that the distributions of lengths or other variants within a trawl can be treated as multi-nominal, but with different multi-nominal distributions in separate trawls. Assuming that the proportions in log space are independent and that the variances are known, the log-likelihood, ignoring constants, is given by

$$F_{GS} = \sum_{k}^{ng} \sum_{j}^{d+1} \frac{1}{\omega_j^2} \left[y_{k,j} - \log \frac{p_{k,j}}{g(p)} \right]^2$$

where ng is the number of gonad samples, $d+1$ is the number of proportions, ω_j is the standard deviation for proportion j, $y_{k,j} = \log \frac{x_{k,j}}{g(x)}$, x is the sample proportion, $g(x) = \left(\prod_{j}^{d+1} x_j \right)^{\frac{1}{d+1}}$, and p is the model estimate of the proportions given by $f_j(t_k) \Big/ \sum_{l} f_l(t_k)$.

The objective function was set into a sum of squares formulation because estimation of variances at the same time as other parameters tends to be unstable, especially at the start of the search. Also, the variances can be estimated outside the model and are used to weight the various data (and for simulations to get the variances of turnover).

In the optimisation procedure, if trial values of *a*, *b*, or *c* were such that *a=b* or *a=c*, or *b=c*, then trial values were changed by a random amount. Similarly for *a2*, *b2* and *c*. Estimates of *a, b, a2, b2,c, c2, B* were found by minimizing *F* with set values of t_1, *ta*, t_c , t_{c2} , t_0. Estimates of t_1, *ta*, t_c , t_{c2} , t_0 were found from a linear search where each one was varied singularly. Each was varied in turn. The sequence was repeated until the estimates did not vary from one iteration to the next.

Significance testing for selecting terms to include in the model

A forward selection procedure was used to add parameters to the model. The base model used the parameter set Mc = {*a, b, B,* t_0}. Other potential parameters were available in the set Vtry = {*(a2, b2, ta), (r1,* t_1*), (c,*t_c*),(c2,*t_{c2}*)*}. The element, *(c,*t_c*),* means that both *c* and t_c are used together as a unit, i.e., two extra parameters are fitted.

The method used was as follows.

1. Estimate the parameters using the set Mc.
2. Find the element in Vtry, Vs, that when added to Mc gave the largest reduction in the log-likelihood.
3. Generate 19 simulated data sets using the estimated parameters in Mc. For each dataset, find the reduction in the log-likelihood from using parameters Mc to that for using {Mc, Vs}.
4. If the observed reduction in the log-likelihood is greater than all 19 simulated values, then adding Vs is statistically significant. Add Vs to Mc and remove it from Vtry.
5. Repeat steps 1 to 4 until either Vtry is empty or the test in 4 fails.

The test in step 4 is a one sided test at the 5% level. Hope (1968) shows that a simulated test procedure based on the observed value being greater (or less) than (N-N*0.05) of the (N-1) simulated values (N and N*0.05 must be integers). The minimum of N=20 is used. As N increases so too does the power of the test. Loss in power, compared to the uniformly most powerful test, is only a problem for moderate differences from the hypotheses being tested and when the degrees of freedom is low. Having 15 degrees of freedom gave about 80% efficiency for N=20 in the simple situations investigated by Hope (1968). More than 15 degrees of freedom are present and so using N=20 seems an effective compromise between computer time and efficiency.

Estimation of variance in the proportion of macroscopic gonad stages

An approximate estimate of the standard error for the proportions of gonad stages (mature, ripe, and spent) was needed to scale these data in the objective function. Primarily this was to scale each stage relative to the other, as the objective value from the gonad data was multiplied by a given constant so that neither biomass or gonad data dominate in the estimation procedure.

The gonad proportion data were treated as a logistic-normal distribution so residuals had to be generated after the data had been logistically transformed. Residuals were the difference between the observed transformed proportions and those from a smooth trend for each stage. This uses Turkey's (1977) method of a running median over 5 values (i.e., 4(3RSR)2H, twice). This method treats the values as if they were from a time series equally spaced in time. Although this not the case for our sampling study, it was adequate for our purpose. The benefit was that it was based on medians and did not seem to overly flatten the peak in the ripe proportion which other smoother tend to do.

Two data sets were used; one from 1999 (this study) and another from an egg survey in 1996 (Francis *et al.* 1997). Proportions over 0.99 and below 0.01 were set to these values and the sample proportions re-normalised. This is necessary to allow the log transform to work. The number of points for males was 25 (10 from1996 and 15 from 1999), and for females, 25 (10 for 1996 and 15 for 1999). A potentially confusing point here is that the females were grouped so that stages 4 and 5 were the ripe stage in the model. This grouping was carried out early on in the analysis and showed similar estimates for the standard deviations to that from the male data. The analysis using female data where the model ripe stage is just stage 5, is given below. Separate trend lines were fitted to each sex and the resultant residuals combined.

The estimate of the standard deviations for the proportion of mature, ripe, and spent gonad stages were 0.66, 0.29, and 0.59. As there was little difference between mature and spent standard deviations, an average was used for these, i.e., 0.62.

The amount of extra variance over that for a multinomial distribution was substantial. For a proportion of 0.5, the binomial standard error is 0.5; for a sample size of 10, it is 0.16; and for a sample size of 100 it is 0.05. Back-transforming the estimated logistic standard errors above gave a standard error of 0.16 for a proportion of 0.5, equivalent to a binomial sample size of 10. As most of these samples had 50 or more fish in

them, the major error source was between trawls and not from sampling the catch of a particular trawl.

The distribution of the residuals was estimated using the S function "density" (Wegman 1972) using a gaussian window of width 1.5 (a small simulation study showed that for 150 samples (2 sexes x 25 samples x 3 gonad stages). The estimated distribution from the simulated sample data was close to the normal distribution curve. Figure 13 shows that the standardised residuals have a distribution that is close to, but not exactly, normal, with too much density at the centre. The correlations of the residuals within a sample are low (less than 0.20) so that treating the logistic transforms of the proportions as independent should give little trouble.

Thus, the proposed method of treating the proportions as independent logistic-normal variables in the fitting procedure (i.e., the proportions of mature, ripe, and spent within one sample are independent of each other in the logistic scale), should be satisfactory.

When the female data were divided so that the model ripe stage was just the stage 5s, the estimate of the standard deviations for the proportion of mature, ripe, and spent gonad stages were 0.56, 1.1, and 0.29.

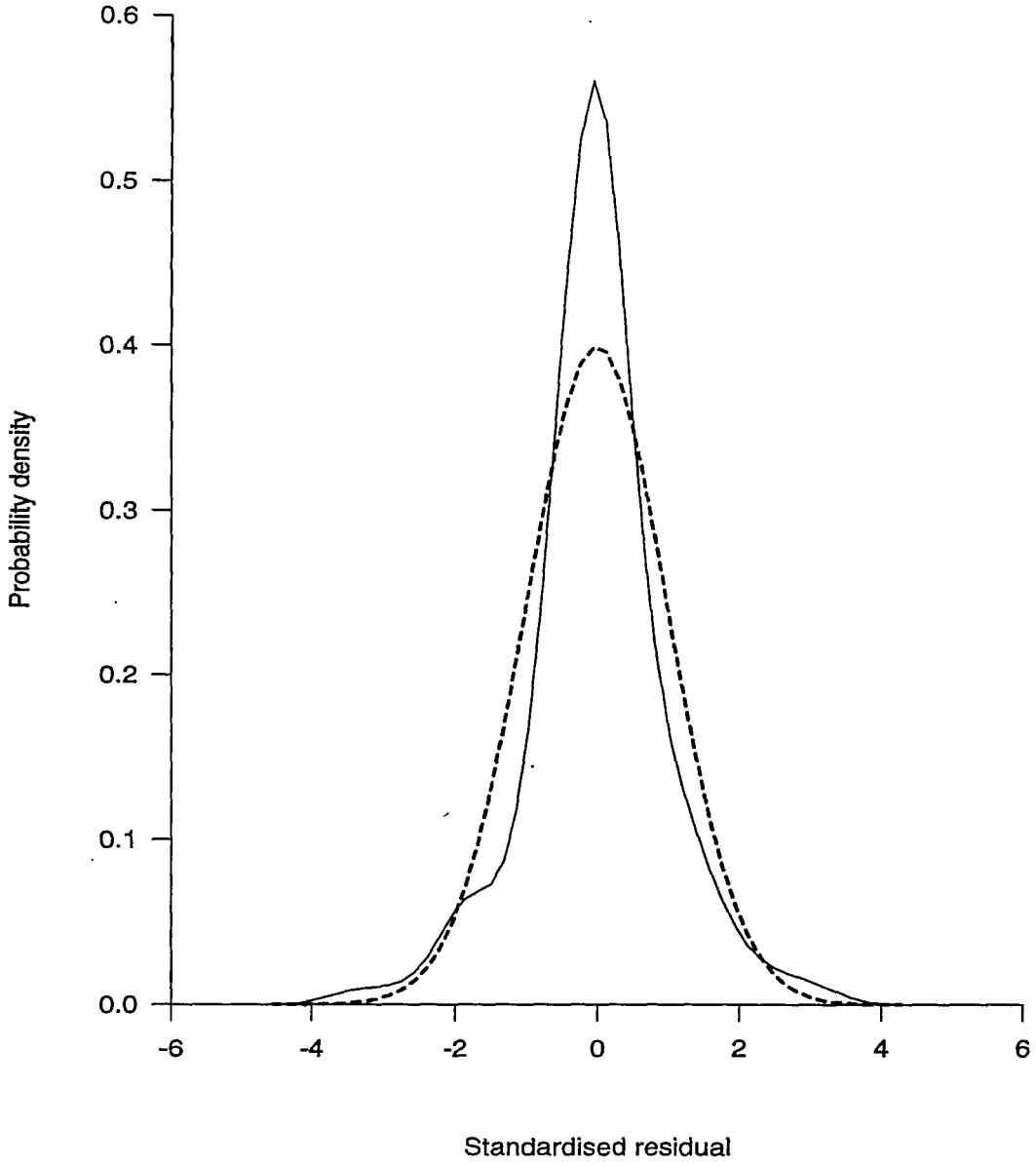

Figure 13: Comparison of the distribution of the standardised residuals under a logistic transformation of the proportions of gonad stages (solid line) compared to the standard normal distribution (dotted line). Male and female data where the female's "ripe" stage was stage 4 and 5.

Results

Three stage spawning dynamics and turnover model

Males

Using the 1999 gonad data, the selected model used the additional parameters, *c2* and t_{c2} (model 2 in Table 4) and because *r1* or *c* were not selected, no turnover occurs with this model (Figure 14). The *c.v.*'s of the estimated values for *a, b, B,* t_0, and t_{c2} were acceptable but *c2* was poorly estimated (Table 4). The highest correlations between estimated values were for t_0 and *a* (0.5) and t_{c2} and *c2* (0.85). The simulations used to estimate variance showed that these parameters are estimated with little bias, except for *c2*.

Table 4: Male spawning dynamic model selection using 1999 biomass estimates and gonad data. Increase in the log-likelihood as observed in the real data (Obs) and the largest in 19 simulations (Sim) and the parameter estimates. Parameter "B" has been converted into total biomass (t) rather than reporting the biomass at time t0. *C.v.*'s (%) are given for the selected model (model 2). "–" means that the parameter was not used or that the log-likelihood increase was not relevant

	Increase in log- likelihood		Parameter estimate												
Model	Obs	Sim	*a*	*b*	*B*	*c2*	*a2*	*b2*	*r1*	*c*	t_0	t_{c2}	*ta*	t_1	*tc*
1	–	–	0.34	0.16	1905	–	–	–	–	–	18	–	–	–	–
2	29.8	27.7	0.34	0.16	2168	1.65	–	–	–	–	18	46	–	–	–
3	6.1	8.8	0.51	0.19	2397	0.22	–	–	44.51	–	18	39	–	37	–
C.v.	–	–	10	9	6	107	–	–	–	–	2	9	–	–	–

The selected model captures the major features in the data (Figure 14), however the size of the residual for the gonad data are too large and the model is slightly biased in some places.

The general size of the residuals can be gauged from the estimated *c.v.*s using the residuals from the model fit. For the *c.v.* of the biomasses (i.e., that using 1 transect), the estimate from the model fit was 54%, quite close to the 50% estimated from the acoustic transect data. The estimated standard errors for the gonad stage proportions from the residuals in the model fit were 0.7, 0.7, and 0.4. Compared to the values used in the analysis, 0.62, 0.29, and 0.62, these model fit estimates seem adequate except that for the ripe proportions which seem to have some difficulties in fitting to the model over and above sampling error. The simulations showed that the median value of the estimated standard deviation was 0.40 and so the spent proportions fit adequately. However an estimate of 0.7 in the simulations was unlikely. As a result, both the proportion of maturing and ripe stages fit poorly relative to sampling error. Either the model is too simplistic or the values used for the standard deviation of the gonad proportion are too low.

When the proportion data are plotted over the trajectory expected from the selected model (Figure 14), the main mis-fit occurs at the peak in the ripe proportion. Between days 22 and 30, there are 7 points and, for all, the ripe proportions are on or above the model curve while the spent proportions are on or below it. This systematic mis-

fitting shows that, in parts, the model is slightly biased. Adding extra parameters *a2*, *b2*, and *ta* can fix this systematic mis-fitting, but it is not statistically significant at the 5% level.

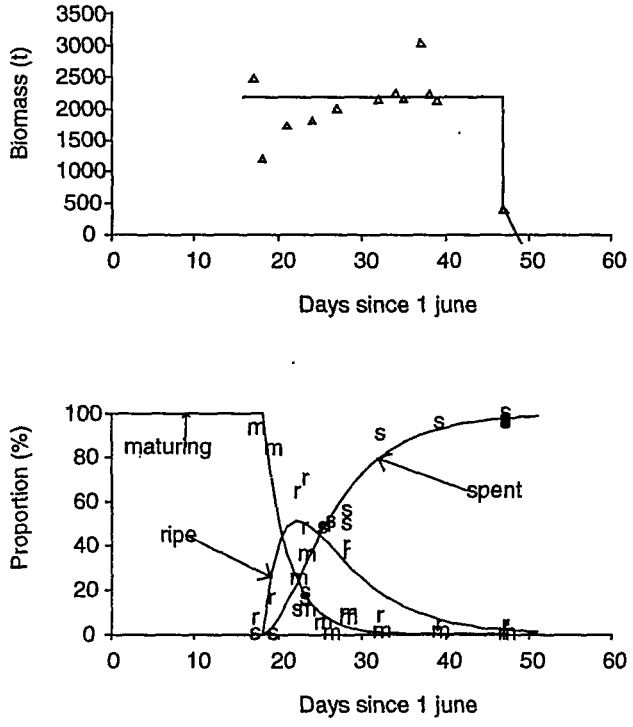

Figure 14: Spawning dynamics of males from the estimated model (lines) and observed data. 1999 biomass estimates (triangles) and gonad data ("m" mature, "r" ripe, and "s" spent).

Table 5: Male spawning dynamic model selection using 1999 biomass estimates, but using the 1996 gonad data. Increase in the log-likelihood as observed in the real data (Obs) and the largest in 19 simulations (Sim) and the parameter estimates. Parameter "B" has been converted into total biomass (t) rather than reporting the biomass at time t_0. *c.v.*'s (%) are given for the selected model (model 2). "–" means that the parameter was not used or that the log-likelihood increase was not relevant

	Increase in log- likelihood		Parameter estimate												
Model	Obs	Sim	*a*	*b*	*B*	*c2*	*a2*	*b2*	*r*	*c*	*t0*	*tc2*	*ta*	*t1*	*tc*
1	–	–	0.3	0.12	1904	–	–	–	–	–	17	–	–	–	–
2	29.8	15.1	0.3	0.12	2167	0.21	–	–	–	–	17	39	–	–	–
3	4.9	7.7	0.46	0.12	2397	0.22	–	–	44.84	–	17	39	–	37	–
C.V.	–	–	7	7	6	97	–	–	–	–	0	8	–	–	–

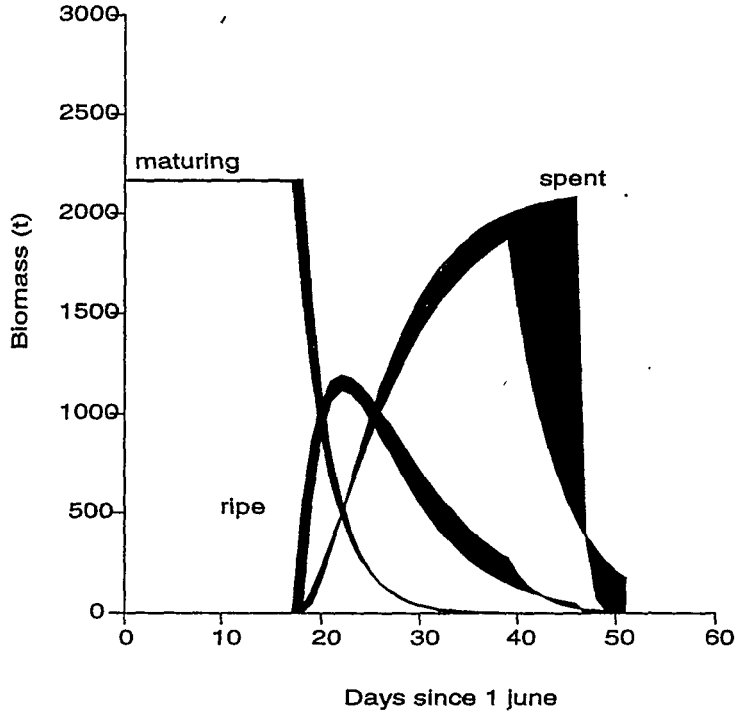

Figure 15: Comparison of the male selected models using 1999 gonad data with that using 1996 gonad data. The difference between the models are shown by the filled in areas.

Using the 1996 gonad data gave the same model as that for the 1999 gonad data (model 2 in Table 5), but with a t_0 that was earlier by 1 day and which was not statistically significant. Compared to the overall length of spawning, the differences between them are minor (Figure 15). A different t_{c2} was selected with the 1996 gonad data, but this parameter is poorly estimated within the last biomass estimate and the

visual estimate, between which both estimates fall, i.e., the differences between the curves at the far right hand end is not significant. This shows that the male parameters do not vary between the two years.

Using the alternative biomass estimates added no new insights or altered interpretations, except that they are more consistent with the plateau predicted by the selected model (Figures 14 & 15). For simplicity, results using the alternative estimates have not been given.

Females

Using the 1999 gonad data, the selected model used the additional parameters, *c2* and t_{c2} (model 2 in Table 6) and because *rl* or *c* were not selected, no turnover occurs with this model (Figure 16). The *c.v.*'s of the estimated values for *a*, *B*, t_0, and t_{c2} were acceptable, that for *b* adequate, but *c2* was poorly estimated (Table 6). The highest correlations between estimated values were for t_0 and *b* (0.7) and t_{c2} and *c2* (0.9). The simulations used to estimate variance showed that these parameters are estimated with little bias, except for *c2*.

Table 6: Female spawning dynamic model selection using 1999 biomass estimates and gonad data. Increase in the log-likelihood as observed in the real data (Obs) and the largest in 19 simulations (Sim) and the parameter estimates. Parameter "B" has been converted into total biomass (t) rather than reporting the biomass at time t_0. *c.v.*'s (%) are given for the selected model (model 2). "–" means that the parameter was not used or that the log-likelihood increase was not relevant

	Increase in log- likelihood		Parameter estimate												
Model	Obs	Sim	*a*	*b*	*B*	*c2*	*a2*	*b2*	*rl*	*c*	t_0	t_{c2}	*ta*	t_1	t_c
1	–	–	0.11	0.13	874	–	–	–	–	–	20	–	–	–	–
2	29.9	7.8	0.11	0.13	995	0.21	–	–	–	–	20	39	–	–	–
3	6.5	7.6	0.14	0.13	1107	0.22	–	–	22.17	–	20	39	–	37	–
C.v.	–	–	10	29	6	90	–	–	–	–	4	9	–	–	–

The selected model captures the major features in the data (Figure 16), although there appears to be one outlier on day 39. The general size of the residuals can be gauged from the estimated *c.v.*s using the residuals from the model fit. For the *c.v.* of the biomasses (i.e., that using 1 transect), the estimate from the model fit was 54%, close to the 50% estimated from the acoustic transect data. The estimated standard errors for the gonad stage proportions from the residuals in the model fit were 0.7, 1.2, and 0.6. The simulations showed that the median value of the estimated standard deviation was 0.55, 0.98 and 0.13 and given the distribution of estimates, the spent proportions fit poorly relative to sampling error (the value 0.6 is an extreme value in the simulations). Removing the gonad data for day 39 reduces the spent estimated standard deviation to 0.4 which is well within the distributions of estimated values.

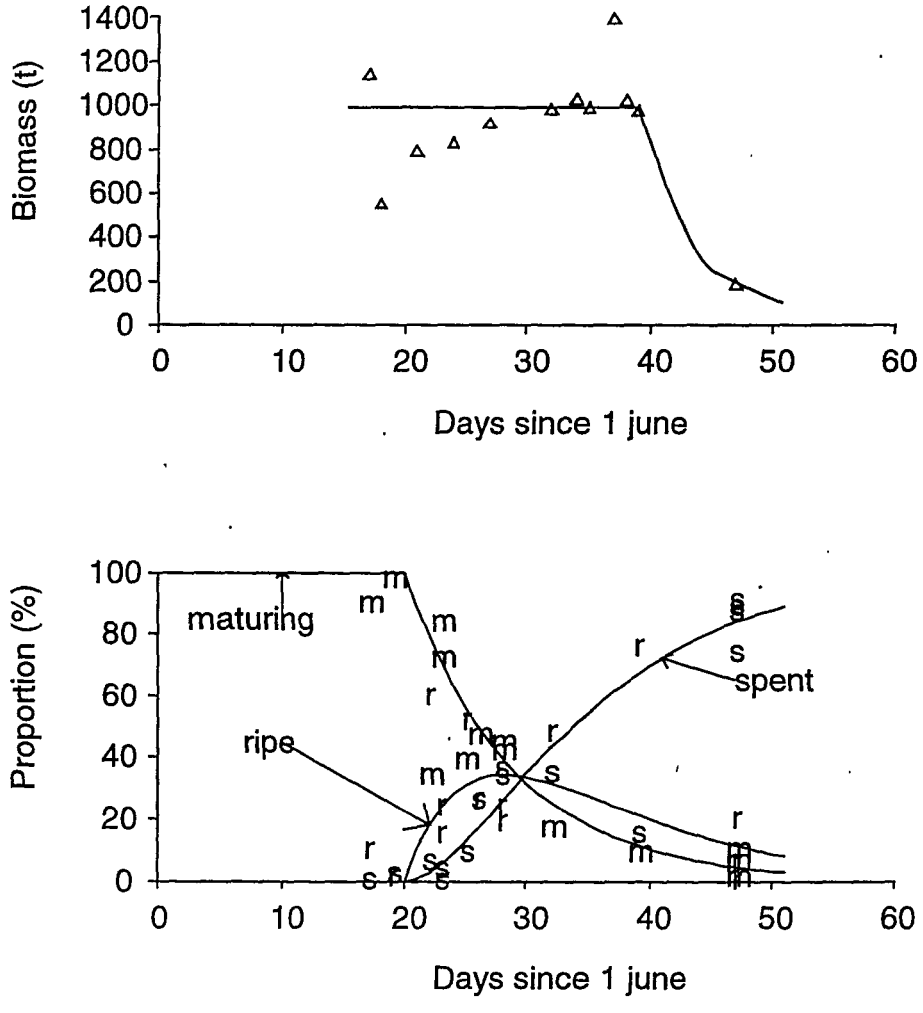

Figure 16: Spawning dynamics of females from the estimated model (lines) and observed data. 1999 biomass estimates (triangles) and gonad data ("m" mature, "r" ripe, and "s" spent).

Table 7: Female spawning dynamic model selection using 1996 biomass estimates, and using the 1996 gonad data. Increase in the log-likelihood as observed in the real data (Obs) and the largest in 19 simulations (Sim) and the parameter estimates. Parameter "B" has been converted into total biomass (t) rather than reporting the biomass at time t_0. c.v.'s (%) are given for the selected model (model 2). "–" means that the parameter was not used or that the log-likelihood increase was not relevant

	Increase in log- likelihood		Parameter estimate												
Model	Obs	Sim	*a*	*b*	*B*	*c2*	*a2*	*b2*	*rl*	*c*	t_0	t_{c2}	*ta*	t_1	t_c
1	–	–	0.08	0.14	874	–	–	–	–	–	17	–	–	–	–
2	29.9	13.2	0.08	0.14	995	0.21	–	–	–	–	17	39	–	–	–
3	6.3	12.4	0.1	0.15	1107	0.22	–	–	21.98	–	17	39	–	37	–
C.V.	–	–	9	9	6	101	–	–	–	–	2	9	–	–	–

Using the 1996 gonad data gave the same model as that for the 1999 gonad data (model 2 in Table 7), but with different values of a and t_0 (statistically significant). Again, compared to the overall length of spawning, the differences between them are minor (Figure 17), with spawning starting 3 days earlier in 1996, but with the latter part of the spent build-up being approximately the same.

Thus, female parameters may vary between years, but the differences appear to be minor, at least between the two.

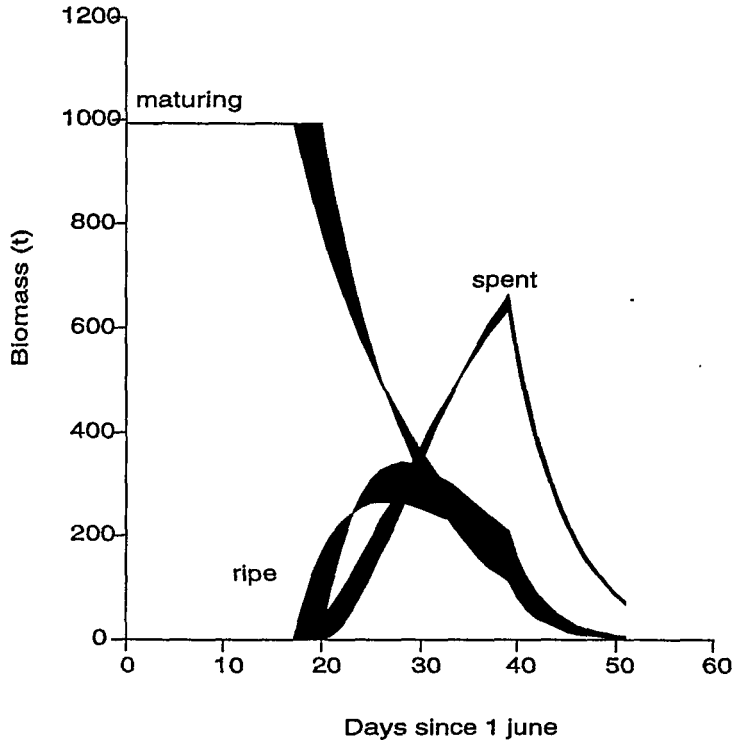

Figure 17: Comparison of the female selected models using 1999 gonad data with that using 1996 gonad data. The difference between the models are shown by the filled in areas.

Histological data

Development in the macroscopic gonad stages is approximately related to the proportion of POF's obtained from the histological data but there is considerable overlap of this proportion between the stages (Table 8). Macroscopic stages 3 and 4 have POF proportions mainly below 15%, stage 5 and 8 have POF proportions 15 to 85%, and stage 6 has proportions mainly over 85%.

Macroscopic stages 3 and 4 are better differentiated in terms of the proportions of GVM oocytes as a total of active oocytes (GVM and M), where stage 3 gonads have a higher proportion of GVM than present in stage 4s. Again there is sizeable overlaps in the distributions of GVM proportions.

The proportions do not correct for the different detection probabilities for different sizes of the GVM and M oocytes and POF's. This omission will affect some values, but the overall trend will be the same.

Table 8: Median POF as a proportion (%) of the sum of POF and active oocytes by macroscopic stages 3 to 8, and the number of gonads in each macroscopic stage (n)

Macroscopic		POF proportion						
stage	n	0	0+ – 14	14+ – 39	39+ – 85	85+ – 89	89+ – 99	99+ – 100
3	89	42	25	24	9	0	0	1
4	137	24	37	25	10	0	2	1
5	99	2	14	24	39	3	16	1
6	38	0	0	8	21	8	37	26
8	43	2	5	30	58	0	5	0

Table 9: GVM as a fraction of the active oocytes by macroscopic gonad stages 3–8, the number of gonads with active oocytes recorded in each macroscopic stage (n), and the median proportion of active oocytes to the sum of POF and active oocytes. [Note that not all gonads had GVM and M oocyte numbers recorded separately so that sample numbers do not match with those in the table 8]

Macroscopic		Active	POF proportion				
stage	n	(%)	0	0+ – 19	19+ – 79	79+ – 99	99+ – 100
3	68	90	1	1	12	29	56
4	107	88	7	13	40	24	16
5	82	58	29	21	23	13	13
6	19	15	26	0	11	16	47
8	39	50	26	8	8	8	51

Clearly, some gonads staged macroscopically as 3 and 4 have significant proportions of POF's when the histological sections are examined (Table 8), but it is unclear if this means that they have partially spawned, although this is the obvious interpretation. For the macroscopic staging to represent a sequence where gonads pass through each macroscopic stage from 3 to 6, the presence of POF's means that either staging is inaccurate or that macroscopic stage 3 and 4 gonads hold free eggs which are overlooked or are somehow lost during the catching process. The latter is unlikely given that macroscopic stage 5 orange roughy gonads with freely running eggs are observed when examined at sea.

POF proportions within a macroscopic stage changes over the course of spawning (Table 10). Generally, the first and third quartiles of the POF proportions increase over time so that macroscopic stage 3 gonads start with less than 10% POF's early on, but have up to 38% later in the spawning season. A similar pattern occurs for macroscopic stage 4 gonads. Most macroscopic stage 5 gonads have some POF's with an increasing proportion over time. The exception is spent fish (macroscopic stage 6), which have high proportions of POF's when such fish first begin to appear, but lower proportions can occur later in the season. One interpretation of this pattern is that individual fish have a cycle where batches of eggs are brought through from stage GVM to M (hydrated), are released within the ovary as free eggs, and then subsequently spawned. For some fish, batches are well separated initially so that a spawned fish can be macroscopic staged as a 3 because it has not hydrated another batch of eggs, or macroscopic staged as a 4 if it has some hydrated eggs. Over the course of spawning, the batches overlap of the cycle rate quickens, so that macroscopic stage 3 fish disappear and the proportion of macroscopic stage 5 fish dominate that of macroscopic stage 4.

With the apparent complexity of oocyte development, macroscopic staging could be inaccurate as an indicator of the underlying gonad development and so only follows microscopic development in a coarse way.

Table 10: First (Q1) and third (Q3) quartiles of POF percentage by macroscopic female stages by dayof sampling. "–" sample size (n) less than 5

Day since	Stage 3			Stage 4			Stage 5			Stage 6		
1 June	n	Q1	Q3	n	Q1	Q3	n	Q1	Q3	n	Q1	Q3
17	20	0	10	7	0	1	0	–	–	0	–	–
19	23	0	0	23	0	9	5	0	8	0	–	–
22	20	4	35	39	1	34	0	–	–	0	–	–
23	3	–	–	10	0	5	8	11	35	0	–	–
25	1	–	–	7	0	8	8	16	48	0	–	–
26	6	0	0	14	0	13	6	3	31	5	87	98
28	15	0	29	23	3	31	8	13	42	17	85	100
32	1	–	–	10	0	41	23	25	51	7	34	95
39	0	–	–	3	–	–	38	55	97	0	–	–
47	0	–	–	1	–	–	3	–	–	9	66	93

The progress of spawning in terms of the POF proportions is shown in Figure 18 using a number of quantiles of the POF proportion distribution at each sample date. The leading front of spawning (95 percentile) reached 100% POF's at day 26 and took about 12 days to attain this level (assuming that the curve can be linearly extrapolated back to the time axis). The median of the distribution took 20 days to reach 80% level where it then seems to remain constant. Lower quantiles progressively started later and stopped (about day 39) to a lower level.

Assuming that the presence of POF's indicates spawning, some spawning had occurred at the start of the sampling on 17 June (Figures 18 & 19). Spawning that leads to a steady progression in the distribution of POF's starts on the 18 to 19 June (Figure 19) with most fish having started by the 18 June. Spawning progresses steadily after 26 June through to 9 July when larger proportions of completely

spawned out fish are present. Another way to look at it is with the 25 and 75 percentiles in Figure 18. These percentiles enclose a block that contains 50% of the fish. This block starts spawning over an 8 day period from 18 June (75 percentile) through to 26 June, after which the block progresses through spawning at about the same rate over the next 13 days to 9 July (as judged by similarity in the slopes of the 25 and 75 percentiles). Thus, spawning is synchronised to the extent that the same point in spawning development is spread over about 8 days, rather than weeks or months in some other species. Figure 19 suggests that individuals spawn in a series of batches.

The POF proportion also showed little evidence of a large influx of maturing fish (Figure 18) which would show itself as a sudden dip in the median and other quantile curves. However, from days 22 to 25, the quantiles are reasonably flat, which may suggest some influx over this period. In Figure 19, the distribution of POF's on 23 June shows more fish with zero POF's, but the fish with POF's are mostly below 35%, rather than being up to 50 or 60% as expected by the sample on the previous day. Thus, this influx may be more apparent than real as a result of a sampling anomaly.

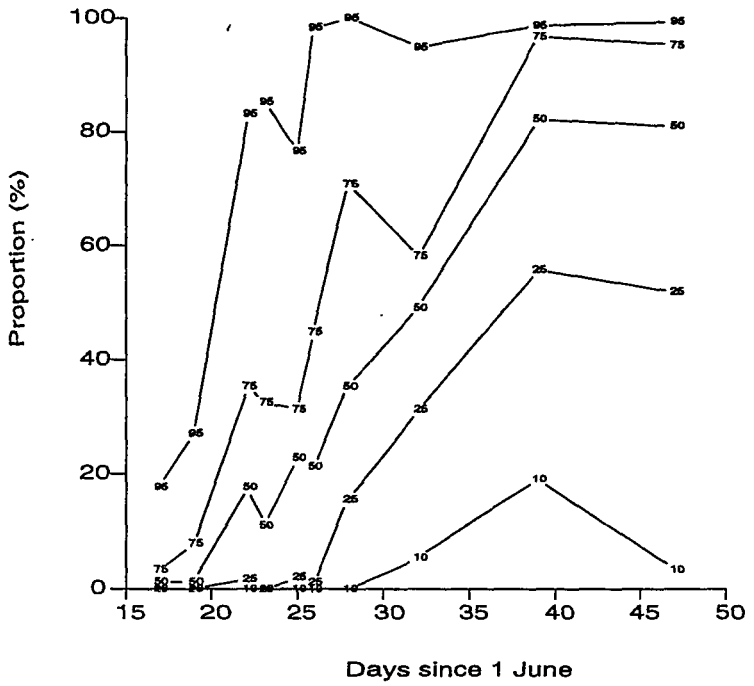

Figure 18: quartiles of the distribution (10,25,50,75,95%) of the POF proportion by time.

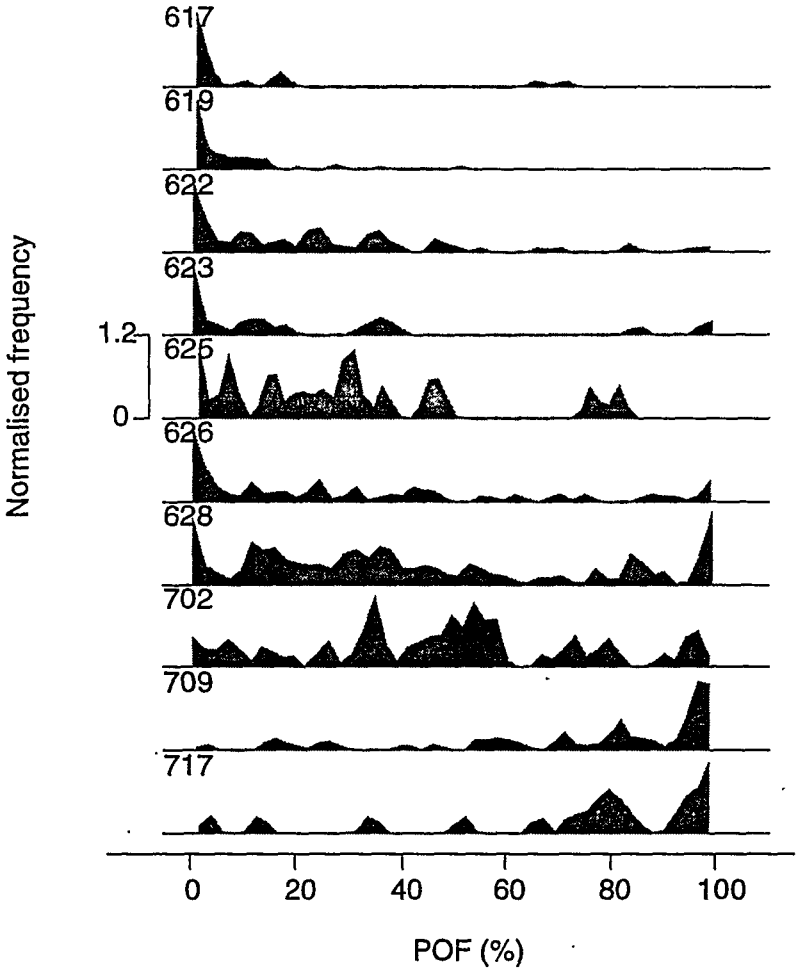

Figure 19: Distribution of the POF proportions by date. The frequency has been normalised so that the maximum is 1. Dates are given as 'mdd', where month m is 6 or 7, and dd is the day within the month.

Discussion

The macroscopic spawning model is primarily concerned with describing the changes in the macroscopic staging and biomass data. In general terms both the male and female models carried this out. Data on the build-up and decay of biomass were scarce and so this aspect of spawning could not be satisfactorily investigated. The start of spawning for females correlates well with the 1996 gonad data (day 17 for both years), but females began spawning 2 days after males in 1999 (day 20 and 18). Zeldis et al. (1997a) found that planktonic eggs first appeared when running ripe female fish (gonads condition macroscopic stage 5) started to occur. This suggests that male spawning should tie in with the appearance of females with gonads in macroscopic stage 5. While the 1996 models data shows this synchronisation, the 1999 model is askew by 2 days. The estimated rates of spawning (b) for both sexes were similar and implied a mean spawning time for an individual of about 6 to 8 days (i.e., $1/b$). Similar rates of spawning for both sexes is what one might expect.

Females can be analysed using ripe and running ripe as the second ("ripe") stage. For the 1999 gonad data, the same model was selected as that used previously, but with a t_0 of 16 and a b estimate of 0.065 (mean time to spawn of 15 days). Thus, females start spawning before males by 2 days (1999), but spawn at half the rate of males. For the 1996 gonad data, the selected model uses the additional parameters $r1$, t_1, and $a2$, $b2$, and ta, where t_0 was estimated as 9 and ta as 24. This model has a low spawning rate from day 9 to 24, and a higher rate thereafter to give an approximate time to spawn of 21 days so that male spawning (as modelled) is not matched at all well. Thus, for the main spawning event, using running ripe as the middle stage for females provides a better fit, particularly for the 1996 gonad data.

The female model can be compared to previous studies which have published a related statistic for the mean time to spawn for active females, (i.e. a gonad macroscopic stage that is one of 4,5, or 8). Zeldis et al. (1997b) called this the mean active time (MAT) and estimated a value of 19 days for the East Cape. Francis et al. (1997) obtained 26 days for the Graveyard in 1996. MAT is consistent with b when using female macroscopic stages 4 and 5 as the stage for ripe. This gave a value of 15 days (i.e., $1/b = 1/.065$) in 1999 and 21 days in 1996. The model estimated MATs are shorter than those given for the Graveyard by Francis et al. (1997), but overlap that given for East Cape. The POF analyses (Figure 18) suggest an estimate of over 12 days (95 percentile) and gives 20 days for the median percentile. However, the model estimate of MAT for 1999 (15) may not be very useful given that the first gonad sample that meets the sampling requirements (i.e., over 500 kg and more than 10 female fish) was on day 17, compared to the start at day 9 for the model using 1996 gonad data. The 1996 data had it's first sample on day 13 and this sample already had 48% of females in the model ripe stage (macroscopic stages 4 and 5).

Naturally, having the models describe the underlying spawning dynamics would be desirable, but this requires that the macroscopic staging be closely linked to the microscopic observations. Unfortunately, such a correlation does not seem to be straightforward and an apparent inconsistency arises as POF's show up in some macroscopic stage 3 and 4 female ovaries. Orange roughy in these two development stages can have over 20% of POF's. Assuming that the presence of POF's indicates spawning, macroscopic stage 3 and 4 females gonads would be expected to have no POF's. Macroscopic stage 3 orange roughy would have mainly GVM oocytes and macroscopic stage 4 fish have various proportions of M oocytes. Thus, gonads have either been mis-assigned or the link between macroscopic and microscopic observations is ambiguous. Although some mis-assignments during macroscopic staging are expected, the levels do seem to be very high (Table 8). Explanations can be speculated on, but this macroscopic / microscopic correlation probably requires further investigations.

All models used in the analyses indicated that there was no turnover and that the biomass on the Graveyard was constant over the period of the surveys (days 17 to 39). The POF proportion also showed little evidence of a large influx of maturing fish (Figure 18). The alternative biomasses (Figure 5) do not suggest any period of increase, but the one's used in fitting the model (Figure 4), could show some increase if the first point was ignored. The extent of possible turnover from this source can be found in model 3 in Tables 4, 5, Figures 14 and 15. These models used a rate of maturing fish arriving onto the Graveyard of 22 t/day for females and 44 t/day for males up to day 37, i.e. most of spawning. The difference in the rates is artificial and is due to male ratio being 70% so that the female biomass is approximately half that of males. This model has no turnover because there is a period, although short (between days 37 and 39), when all the biomass is present. However, at the time of the overall survey on day 24, the biomass was only 76% of the total.

Another way for turnover to occur is for spent fish to leave before spawning has finished. The model selection procedure show little support for such a situation. If turnover was to be present, spent fish leaving early appeared to be the most likely method. This was concluded by Zeldis et al. (1997a) who showed that turnover on the Ritchie Hill was from spent fish leaving early. Using values for the MAT above, a calculation for the time a female stays after completing spawning under turnover conditions could be made. Zeldis et al. (1997a) gave a value of 1.6 to 2.6 days corresponding to a value of c of 0.4–0.6. Such a level of c is likely to have resulted in c and t_c being selected. For other hills, East Cape and the Graveyard in 1996, Zeldis et al. (1997a) and Francis et al. (1997) concluded that no turnover had occurred.

No commercial fishing took place in the study area during the turnover experiment and the only influence in the fish behaviour was the sampling effort by the two survey vessels. As research trawling was required to detect turnover using changes in reproductive condition, the possibility remains that our own sampling effort may have influenced fish behaviour.

Acknowledgements

Special thanks to *Tangaroa, Amaltal Explorer,* and *San Rangitoto* skippers and crew for their input and assistance during the surveys.

We thank George Clement (ORH Management Company), Peter Talley, John Cleal, and Lindsay Copeland (Amaltal Fishing), Tom Birdsall, Ross Bradley, and Morris Prendeville (Sanford Ltd.).

For constructive comments on the text we acknowledge Malcolm Clark.

Data storage:

All trawl and acoustic data are held in the MFish *trawl* and *acoustic* databases. Histological slide samples are stored in the Data Management specimen and data archive store, NIWA, Greta Point.

References

Aitchison, J. 1983: Principal component analysis of compositional data. *Biometika 70.* pp.57–65.

Bell, J.D., Lyle, J.M., Bulman, C.M., Graham, K.J., Newton, G.M., Smith, D.C. 1992: Spatial variation in reproduction and occurrence of non-reproductive adults in orange roughy, *Hoplostethus atlanticus* Collett (Trachichthyidae), from south-eastern Australia. *J. Fish Biol.* 40: 107–122.

Buil, B., Doonan, I.J., Coombs, R.F., 1999: Acoustic estimation of biomass of spawning orange roughy on the Northwest Chatham Rise hills — June-July 1997. Final Research Report, MOF804K. (Unpublished manuscript, held by Ministry of Fisheries, Wellington.) 16 p.

Bull, B., Doonan, I.J., Tracey, D., Coombs, R.F., 2000: An acoustic estimate of orange roughy abundance on the Northwest hills, Chatham Rise, June-July 1999. *New Zealand Fisheries Report 2000/20.* 36 p.

Francis, R. I. C. C., Clark, M.R., and Grimes, P.J., 1997: Calculation of the recruited biomass of orange roughy on the Northwest Chatham Rise using the 1996 Graveyard Hill egg survey (TAN9608). New Zealand Fisheries Research Assessment Document, 97/29.

Hope, A.C.A., 1968: A simplified Monte Carlo significance test procedure. *Journal of the Royal Statistical Society, series B 31.* 582–598.

Pankhurst, N. W. 1988: Spawning dynamics of orange roughy, *Hoplostethus atlanticus,* in mid-slope waters of New Zealand. *Environmental Biology of Fishes, 21*: 101–116.

Pankhurst, N. W., McMillan, P.J., and Tracey, D.M., 1987: Seasonal reproductive cycles in three commercially exploited fishes from the slope waters off New Zealand. *Journal of Fish Biology, 30*: 193–211.

Seber, G.A.F., and Wild, C.J., 1989: Nonlinear regression. JOHN WILEY & SONS, New York

Tukey, J.W., 1977: Exploratory Data Analysis, Chapters 7 and 16, Addison-Wesley, Reading, Massachusetts.

Wegman, E.J., 1972: "Nonparametric Probability Density Estimation", *Technometrics 14*: 533–546.

Wood, B, Tracey, D., Hart, A. 2000: The Northwest Hills on the Chatham Rise. *Seafood New Zealand. February 2000.* 2 p.

Zeldis, J.R. 1993: Applicability of egg surveys for spawning-stock biomass estimation of snapper, orange roughy, and hoki in New Zealand. *Bulletin of Marine Science 53*: 864–890.

Zeldis, J.R., Francis, R.I.C.C., Clark, M.R., Ingerson, J.K.V., Grimes, P.J., and Vignaux, M. 1997a: An estimate of orange roughy, *Hoplostethus atlanticus*, biomass using the daily fecundity reduction method. *Fishery Bulletin 95*: 576–597.

Zeldis, J. R., Francis, R. I. C. C., Field, K. D., Clark, M. R., and Grimes, P. J. 1997b: Description and analysis of the 1995 orange roughy egg surveys at East Cape and Ritchie Bank, and reanalysis of the 1993 Ritchie Bank egg survey. New Zealand Fisheries Research Assessment Document, 97/28. 34 p.

APPENDIX 1

Biomass estimates for turnover mini-snapshots, corrected for differences in transect directions

Brian Bull

Methods

The results of the diurnal experiment showed significant differences between transect paths crossing Graveyard on different directions. The turnover mini-snapshots included various different transect directions: for example, the first snapshot included transects on bearings of 181.6° and 44.5°, the second snapshot 270.0° and 136.7°, and so on. We therefore corrected the mini-snapshot biomasses for the differences in the directions of their transects.

Our method was based on the assumption that estimates of backscatter from single transects on Graveyard were lognormally distributed with mean depending on the day and the transect direction and c.v. constant. The transect effect was assumed not to change if the direction was reversed, i.e. a north-south transect was considered equivalent to a south-north transect. Most transects were carried out along four paths – north-south, northeast-southwest, east-west, southeast-northwest — and the model allowed a separate effect for each of these four directions. The path effect for an intermediate direction was a linear interpolation of the effects of the two closest directions: for example, the path effect for a transect on a 22.5° bearing was the average of the north-south and northeast-southwest effects.

The model was hence

$$\log(y_{s\theta i}) = \mu_s + p_\theta + \varepsilon_{s\theta i}$$
$$\varepsilon_{s\theta i} \sim N(0, \sigma^2)$$

where $y_{s\theta i}$ is the backscatter on the ith transect of snapshot s on a bearing of θ (between 0° and 180°), μ_s is the mean backscatter of snapshot s, p_θ is the path effect for direction θ, defined by

$$p_\theta = \begin{cases} p_0 & \theta = 0^\circ \\ (p_0(45-\theta) + p_{45}(\theta - 0))/45 & 0^\circ < \theta < 45^\circ \\ p_{45} & \theta = 45^\circ \\ (p_{45}(90-\theta) + p_{90}(\theta - 45))/45 & 45^\circ < \theta < 90^\circ \\ p_{90} & \theta = 90^\circ \\ (p_{90}(135-\theta) + p_{135}(\theta - 90))/45 & 90^\circ < \theta < 135^\circ \\ p_{135} & \theta = 135^\circ \\ (p_{135}(180-\theta) + p_0(\theta - 135))/45 & 135^\circ < \theta < 180^\circ \end{cases}$$

such that $p_0 + p_{45} + p_{90} + p_{135} = 0$, and ε is a random error term with variance σ^2.

The parameters of interest are $\{\mu_s\}$ and σ^2. The direction-corrected estimate of mean backscatter for snapshot s is $\exp(\mu_s)$. The *c.v.* of the mean backscatter estimates (and hence of the snapshot biomass estimates) is determined by σ^2:

$$c.v. = \sqrt{\frac{\exp(\sigma^2)-1}{n}}.$$

The $\{\mu_s\}$ and σ^2 parameters were estimated by recasting the model as a linear regression.

Results

Direction-corrected mean backscatter, and SR ORH biomass estimate, by snapshot:

	Mean backscatter		SR ORH biomass (t)	
Snapshot	Raw	Direction-corrected	per unit backscatter	Biomass (t)
Grid 1	59.5	60.7	61.0	3698
Grid 2	34.5	36.9	51.0	1880
Grid 3	51.8	63.8	48.7	3106
Biomass survey	36.6	32.5	72.2	2347
Grid 5	46.7	48.1	62.8	3025
Grid 6	39.6	34.5	79.1	2730
Diurnal day 1	41.3	37.6	79.4	2989
Diurnal day 2	39.7	41.1	79.4	3263
Diurnal day 3	55.9	57.5	79.4	4564
Diurnal day 4	41.0	37.8	79.4	3000
Grid 8	39.0	44.2	79.7	3522

Path effects:

north-south: 0.501
northeast-southwest: -0.167
east-west: -0.387
southeast-northwest: 0.054

(These are similar to the results of the diurnal experiment: north-south high, east-west low, and the diagonals in between.)

And $\hat{\sigma}^2 = 0.146$, leading to a *c.v.* of $39.7\%/\sqrt{n}$. A bit of a reduction from the ~50% we were looking at earlier.

APPENDIX 2

Solution for a three gonad stage (male) as a linear compartmental model

Let the spawning dynamics be given by the following equations

$$\frac{\partial}{\partial t} f_{Mature} = r1 - af_{Ready}$$

$$\frac{\partial}{\partial t} f_{Ripe} = r2 + af_{Ready} - bf_{Ripe}$$

$$\frac{\partial}{\partial t} f_{Spent} = r3 + bf_{Ripe} - cf_{Spent}$$

where f denotes biomass, t is time (days), r's are constant rates of fish moving onto the Graveyard (t.day^{-1}), a, b, and c are constant transfer rates (day^{-1})

In general, the above dynamics can be re-cast into matrix notation involving m compartments (spawning states) so that f is a vector of biomasses in the compartment and the dynamics of shifting from one state to another at time, t, is given by:

$$\frac{\partial f(t)}{\partial t} = Af(t) + r(t)$$

where A is a $m \times m$ matrix of fractional transfer rates between the m compartments, and r is a vector of m input rates, one for each compartment, of which one or more can be zero.

A solution (Seber and Wild, 1989) for f, given that $r(t)=b$, a vector of constants, that A is non-singular, and that initially $f=\xi$, is

$$f = e^{At}(\zeta + A^{-1}b) - A^{-1}b.$$

For the case above, the A matrix is:

$$\begin{bmatrix} -a & 0 & 0 \\ a & -b & 0 \\ 0 & b & -c \end{bmatrix}$$

The following derivation follows that in from section 8.3.1 of Seber and Wild (1989) and requires that $a \neq b \neq c > 0$. The characteristic equation is

$$(-a-\lambda)(-b-\lambda)(-c-\lambda)+0+0=0$$

and the eigenvalues are: $-a$, $-b$, $-c$.

The (adj $(A-\lambda I_3)$) is

$$\begin{bmatrix} (b+\lambda)(c+\lambda) & 0 & 0 \\ a(c+\lambda) & (c+\lambda)(a+\lambda) & 0 \\ ab & b(a+\lambda) & (a+\lambda)(b+\lambda) \end{bmatrix}$$

Substituting $-a$ for λ in column 1, $-b$ for λ in column 2, and $-c$ for λ in column 3 gives the corresponding eigenvectors. Thus,

$$S=\begin{bmatrix}(b-a)(c-a) & 0 & 0\\ a(c-a) & (c-b)(a-b) & 0\\ ab & b(a-b) & (a-c)(b-c)\end{bmatrix}$$

Dividing through columns by common elements simplifies S to

$$S=\begin{bmatrix}(b-a)(c-a) & 0 & 0\\ a(c-a) & (c-b) & 0\\ ab & b & 1\end{bmatrix}$$

Similarly, the row eigenvectors are (using rows 1,2 and 3, and simplifying along rows; note that we could of used row 3 with the eigenvalue, –b, but it is simpler to use row 2 with this eigenvalue)

$$C=\begin{bmatrix}1 & 0 & 0\\ a & (a-b) & 0\\ ab & b(a-c) & (a-c)(b-c)\end{bmatrix}$$

The normalizing constants, $\left({}^{r}c_{j}s_{j}\right)$, for the rows of C are: *(b-a)(c-a), (a-b)(c-b),* and 1. After noting that equation 8.33 in Seber and Wild (1989) has a typo in it, we get

$$S^{-1}=\begin{bmatrix}\dfrac{1}{(a-b)(c-a)} & 0 & 0\\ \dfrac{a}{(a-b)(c-b)} & \dfrac{1}{(c-b)} & 0\\ \dfrac{ab}{(a-c)(b-c)} & \dfrac{b}{(b-c)} & 1\end{bmatrix}$$

A^{-1} is given by $S\Lambda^{-1}S^{-1}$ which gives

$$A^{-1}=\begin{bmatrix}\dfrac{-1}{a} & 0 & 0\\ \dfrac{-1}{b} & \dfrac{-1}{b} & 0\\ \dfrac{-1}{c} & \dfrac{-1}{c} & \dfrac{-1}{c}\end{bmatrix}$$

Let $\xi=(B1, B2, B3)$ be the starting biomasses in each compartment and $b=(r1,r2,r3)$ the constant input rates into each compartment, then evaluating the ${}^{r}s_j^{-1}\{\xi+b/\lambda_j\}s_j e^{\lambda_j t}$ gives

$$j=1 \qquad \frac{B1-r1/a}{(b-a)(c-a)}\begin{bmatrix}(b-a)(c-a)\\ a(c-a)\\ ab\end{bmatrix}e^{-at}$$

$$j=2 \qquad \left(\frac{a(B1-r1/b)}{(a-b)(c-b)}+\frac{B2-r2/b}{c-b}\right)\begin{bmatrix}0\\ (c-b)\\ b\end{bmatrix}e^{-bt}$$

$$j=3 \quad \left(\frac{ab(B1-r1/c)}{(a-c)(b-c)}+\frac{(B2-r2/c)b}{b-c}+(B3-r3/c)\right)\begin{bmatrix}0\\ 0\\ 1\end{bmatrix}e^{-ct}$$

$A^{-1}b$ gives

$$\begin{bmatrix}\frac{-r1}{a}\\ \frac{-(r1+r2)}{b}\\ \frac{-(r1+r2+r3)}{c}\end{bmatrix},$$

The solutions are:

$$f_{Ready}=\{B1-r1/a\}e^{-at}+r1/a$$

$$f_{Ripe}=\left\{(B1-r1/a)\frac{a}{b-a}\right\}e^{-at}+$$
$$\left\{\frac{a(B1-r1/b)}{(a-b)}+(B2-r2/b)\right\}e^{-bt}+(r1+r2)/b$$

$$f_{Spent}=\left\{(B1-r1/a)\frac{ab}{(b-a)(c-a)}\right\}e^{-at}+$$
$$\left\{\frac{(B1-r1/b)ab}{(a-b)(c-b)}+(B2-r2/b)\frac{b}{c-b}\right\}e^{-bt}+$$
$$\left\{\frac{ab(B1-r1/c)}{(a-c)(b-c)}+\frac{(B2-r2/c)b}{b-c}+(B3-r3/c)\right\}e^{-ct}+(r1+r2+r3)/c$$

APPENDIX 3

Estimator for the standard deviation of a proportion in a logistic-normal distribution

Let *ng* be the number of gonad samples, $d+1$ the number of proportions, ω_j the standard deviation for proportion j, $y_{k,j} = \log\frac{x_{k,j}}{g(x)}$, where x is the sample proportion, $g(x) = \left(\prod_j^{d+1} x_j\right)^{\frac{1}{d+1}}$ (Aitchison1983).

Then the y's are of the form: $y_{k,j} = a_j + b_k + \varepsilon_{k,j}$, where b_k is a constant specific to the k-th sample (needed to keep the proportions summing to one). The form of $g(x)$ means that the a_j 's for the k-th sample sum to zero and b_k is given by $-\overline{\varepsilon_k}$, the negative of the mean of the errors over the $p+1$ proportions in log space. If $d+1=3$, then,

$$\left(y_{k,j} - a_j\right)^2 = \left(b_k + \varepsilon_{k,j}\right)^2 = \left(-\overline{\varepsilon_k} + \varepsilon_{k,j}\right)^2$$

$$= \frac{1}{9}\left(\varepsilon_{k,1} + \varepsilon_{k,2} + \varepsilon_{k,3}\right)^2 + {\varepsilon_{k,j}}^2 + \frac{-1}{3}\left(\varepsilon_{k,j}\varepsilon_{k,1} + \varepsilon_{k,j}\varepsilon_{k,2} + \varepsilon_{k,j}\varepsilon_{k,3}\right)$$

Given independent, the expectations are,

$$\mathrm{E}\left[\left(y_{k,j} - a_j\right)^2\right] = \mathrm{E}\left[\frac{1}{9}\left(\varepsilon_{k,1} + \varepsilon_{k,2} + \varepsilon_{k,3}\right)^2\right] + \mathrm{E}\left[{\varepsilon_{k,j}}^2\right] + \mathrm{E}\left[\frac{-2}{3}{\varepsilon_{k,j}}^2\right]$$

$$= \frac{1}{9}\left(\omega_1^2 + \omega_2^2 + \omega_3^2\right) + \omega_j^2 - \frac{2}{3}\omega_j^2$$

$$= \frac{1}{9}\left(\omega_1^2 + \omega_2^2 + \omega_3^2\right) + \frac{1}{3}\omega_j^2$$

For example, when $j=2$, the RHS is, $\frac{1}{9}\left(\omega_1^2 + 4\omega_2^2 + \omega_3^2\right)$.

Summing the $\left(y_{k,j}-a_j\right)^2$ over samples (k and j) and setting in matrix form gives $z = A\omega$, where

$$z=\begin{bmatrix}\sum_{k=1}^{ng}\left(y_{k,1}-a_1\right)^2\\ \sum_{k=1}^{ng}\left(y_{k,2}-a_2\right)^2\\ \sum_{k=1}^{ng}\left(y_{k,3}-a_3\right)^2\end{bmatrix}$$

$$A=\frac{ng}{9}\begin{bmatrix}4 & 1 & 1\\ 1 & 4 & 1\\ 1 & 1 & 4\end{bmatrix}, \text{ and}$$

$$\omega=\begin{bmatrix}\omega_1\\ \omega_2\\ \omega_3\end{bmatrix}$$

The estimate of ω is given by $A^{-1}z$, .i.e.,

$$\frac{1}{18}\begin{bmatrix}5 & -1 & -1\\ -1 & 5 & -1\\ -1 & -1 & 5\end{bmatrix}\frac{9}{ng}z$$